INFORMATION TO USERS

This manuscript has been reproduced from the microfilm master. UMI films the text directly from the original or copy submitted. Thus, some thesis and dissertation copies are in typewriter face, while others may be from any type of computer printer.

The quality of this reproduction is dependent upon the quality of the copy submitted. Broken or indistinct print, colored or poor quality illustrations and photographs, print bleedthrough, substandard margins, and improper alignment can adversely affect reproduction.

In the unlikely event that the author did not send UMI a complete manuscript and there are missing pages, these will be noted. Also, if unauthorized copyright material had to be removed, a note will indicate the deletion.

Oversize materials (e.g., maps, drawings, charts) are reproduced by sectioning the original, beginning at the upper left-hand corner and continuing from left to right in equal sections with small overlaps.

Photographs included in the original manuscript have been reproduced xerographically in this copy. Higher quality 6" x 9" black and white photographic prints are available for any photographs or illustrations appearing in this copy for an additional charge. Contact UMI directly to order.

Bell & Howell Information and Learning
300 North Zeeb Road, Ann Arbor, MI 48106-1346 USA

UMI®
800-521-0600

The Study of β-Cyclodextrin Interactions with Sugars Using "Inhibition Kinetics" And The Bromination of Pyrimidine Derivatives

Isabelle Turner

A Thesis

in

The Department

of

Chemistry and Biochemistry

Presented in Partial Fulfilment of the Requirements
for the Degree of Master of Science at
Concordia University
Montréal, Québec, Canada

August 1999

ABSTRACT

The Study of β-Cyclodextrin Interactions with Sugars Using "Inhibition Kinetics"

And The Bromination of Pyrimidine Derivatives

Isabelle Turner

PART I: The binding of β-cyclodextrin (β-CD) with sugars was studied using "inhibition kinetics". The rates of hydrolysis of trimethyl orthobenzoate and benzaldehyde dimethyl acetal in acidic solution were monitored using a single beam stopped-flow spectrophotometer. Both substrates exhibit saturation kinetics and 1:1 binding with β-CD, and the rates of hydrolysis are retarded by the cyclodextrin, in agreement with earlier studies. The retarded rates of hydrolysis in the presence of β-CD are modulated by the addition of guests that bind to the CD, and "inhibition constants" (K_i) may be determined. Several aldoses were studied. Pentoses were found to bind modestly to β-CD (K_i = 100 - 1000 mM) and hexoses hardly bind at all (K_i > 500 mM). The results obtained with the two probe reactions agree well with each other, and the K_i values are compared to the disparate values in literature.

PART II: The aqueous bromination of 2-aminopyrimidine (2-AP) involves two major steps, and the first step forms an addition product, an intermediate that was previously observed by NMR. The second step, which is quite slow, involves

elimination of water from the intermediate to yield the 5-bromo derivative. The focus of this investigation was on the initial fast step to try to discover how the intermediate is formed. The kinetics of the bromination of 2-aminopyrimidine and several related derivatives have been studied using a stopped-flow apparatus. The mechanisms were investigated by constructing pH-rate profiles for each compound. The pH-rate profiles for 2-aminopyrimidine and 1,2-dihydro-2-imino-1-methyl-pyrimidine (M2A) demonstrate the complexity of these reactions and the evidence that more than one mechanism is involved. This statement is especially true for the latter compound where mixed orders of reactions were found. For comparative purposes the kinetics of bromination of 2-amino-4,6-dimethyl-pyrimidine (2-ADP), 2-aminopyridine (2-APy), 2-dimethylaminopyridine (2-DAPy), aniline and *N,N*-dimethylaniline were also studied.

Acknowledgements

I would like to thank my supervisor Professor Oswald S. Tee for his patience and his support. I am grateful for his teachings of both life and science. Thank you for being such a good pedagogue and above all a patient English teacher.

I am appreciative of Dr. Timothy A. Gadosy and Dr. Joanne Turnbull for readily accepting to be on my committee, even if they knew what they were getting into.

I am pleased to have met and exchanged with a large number of fellow students in the Department of Chemistry and Biochemistry. Several have become friends and I hope to keep in touch. Special thanks to Alexei A. Fedortchenko, Delna Ghadiali, Michael John Boyd, Lee Fader, Araz Jakalian, Michael Harvey and Donald Paquette. Good luck to Paul Loncke, Ogaritte Jennifer Yazbeck, and Doris Badaan in reaching their academic goals.

Finally I could not have completed this thesis without the support and love of my family and friends.

À ma famille:

Michel E. Turner
Louise G. Gladu Turner
Terry R. Turner
Richard W. Arnett

«Tout ce que l'homme pouvait gagner au jeu de la peste et de la vie, c'était la connaissance et la mémoire.»

Albert Camus
La Peste

Table of Contents

List of Figures

List of Schemes

List of Tables

PART I

The Study of β-Cyclodextrin Interactions with Sugars Using "Inhibition Kinetics"

1. Introduction

1.1 Supramolecular Chemistry and Molecular Recognition

During the late sixties a new field was developed, an explosion in the investigations of highly structured complexes with the goal of mimicking enzymes. Supramolecular chemistry is the study of the functions and the structures of supermolecules which are formed during the associations of substrates and receptors.[2] Many biological processes, such as substrate binding to an enzyme, and enzymic catalysis, exploit supramolecular properties.

Following the growing interest in supramolecular chemistry Cram *and coworkers* in 1977, defined the terms to be used in host-guest complexation. Supramolecular complexes were defined as "composed of two or more molecules or ions held together in unique structural relationships by electrostatic forces other than those of full covalent bonds."[1] The forces that are usually involved include Van der Waals, hydrophobic, dipolar and polar interactions. Covalent bonds are excluded since they lead to a molecule instead of a complex. A molecular complex requires a minimum of one host and one guest component. The host is known as "an organic molecule or ion whose binding sites converge in the complex."[1] The guest is therefore "any molecule or ion whose binding sites diverge in the complex."[1] A simple representation of a molecular complex can be seen in Scheme 1.1.

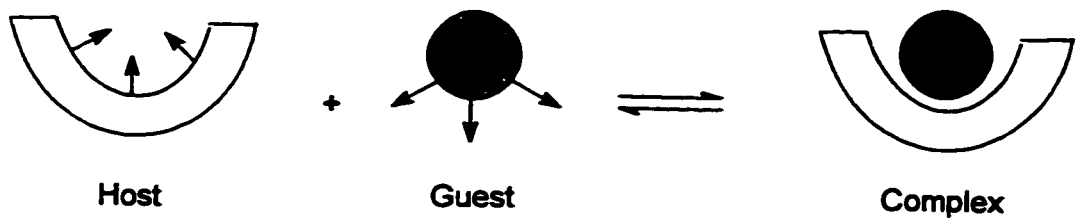

Scheme 1.1 Schematic Represenation of a Molecular Complex. The Host molecule is convergent and the Guest molecule is divergent.

For a guest to bind to a potential host several requirements must be met: both the host and the guest must complement each other *i.e.*, the geometry, size and shape must allow appropriate interactions to occur; the host should have a degree of flexibility and of rigidity to allow the access of the guest to the binding site.[2] When interaction is made possible, the function of the supramolecular complex can be investigated. Functional properties of a supermolecule include catalysis, transport and molecular recognition.[2]

The main requirement of molecular recognition is that the receptor and its substrates be in contact over a large area.[2] In order to satisfy this requirement several factors play a key role. The first factor involves diffusion. Encounters between a host and a guest occur through diffusion. If a complex is formed upon contact, the rate of complex formation is diffusion-controlled. On the other hand, if some adjustments to structure of the host and/or the guest are needed (preorganisation), the rate of complexation will be slower.[6] When the surfaces of both molecules come in contact, multiple weak bonds are formed and will hold until random thermal motions lead to the dissociation of the molecules.[6]

Therefore the second factor involves thermal motions. A general correlation between binding strength and the rate of dissociation is the stronger the binding the slower the rate of dissociation. In the case of a fast rate of dissociation, the total energy of the bonds formed is negligible in contrast with that of thermal motion, the molecules dissociate very rapidly. If the binding is strong, the bond energy is high resulting in a slow rate of dissociation.[6] Preorganisation will play a major role in determining the binding power,[1] this is because by adjusting their structures the molecules enhance the fit and the number of noncovalent interactions. Complementarity will be involved in structural recognition,[1] not only does it increase the number of noncovalent bonds formed, it also increases the area of contact, satisfying the main requirement of molecular recognition.

The third and last factor involves molecular motion. All three kinds of molecular motions are significant in bringing the surfaces of interacting molecules together. These motions are: translational, vibrational and rotational.[6]

Many scientists have contributed to the studies of host-guest chemistry and have elaborated potential applications, some of which are drug design, new analytical and diagnostic procedures, enzyme-analogous catalysis in water, etc...[7] Other researchers focussed on designing and constructing hosts, adding to the list of existing hosts. Common hosts include crown ethers, cryptands and cyclodextrins.

1.2 Cyclodextrins

Cyclodextrins were first discovered from a culture of *Bacillus amylobacter*

grown on a starch medium by Villiers in 1891.[3] Following this discovery, Schardinger was able to isolate a bacillus (*Bacillus macerans*) which yields cyclodextrins upon treatment with starch.[4] Through years of extensive work by various researchers secrets of the cyclodextrins have unfolded revealing their structures and chemical and physical properties.

The reaction of the enzyme cyclodextrinase on starch is relatively specific, forming only a few byproducts.[5] The main products are three different cyclodextrins, α-, β-, and γ-, varying in the number of glucose units as follows: 6 units, 7 units and 8 units (Scheme 1.2). Several methods can be used to isolate them including: gel chromatography, column chromatography, HPLC, etc.[4,5]

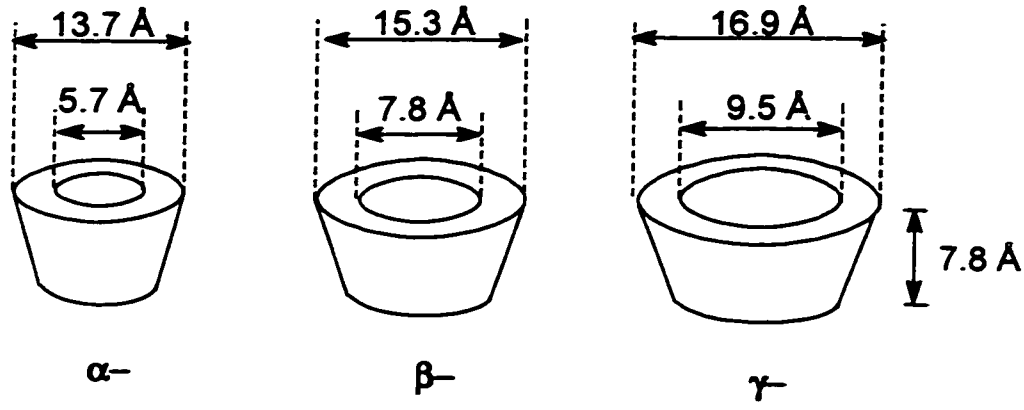

Scheme 1.2 The Molecular dimensions of the Three Different Cyclodextrins (α-, β- and γ-CD).

1.2.1 Structure, Chemical and Physical Properties

The doughnut-shape of CDs is one of their interesting features (Scheme

1.3). This particular shape is allowed because the undistorted D(+)-glucopyranose units in the C1 conformation are attached by α-1,4-linkages.[3,4] A consequence of the C1 conformation is that the secondary hydroxy groups, which are situated on the C-2 and C-3 positions of the glucose units, are located on the larger opening of the CD, and the primary hydroxy groups are located on the smaller side of the CD.[3,4]

The secondary hydroxy groups of adjacent glucose units (C-2 and C-3) are involved in hydrogen bonding, resulting in stabilization of the shape of the molecule and affecting its solubility in water.[3] Secondary hydroxyl groups are fairly rigid and do not rotate whereas free rotation of the primary hydroxyl groups is allowed and they can partially block the cavity by rotating.[4]

The primary characteristic of this torus shape is its cavity. The cavity of CDs are mainly composed of C-H groups and glucosidic oxygens which makes it relatively apolar.[4] The fact that the electron pairs of the glycosidic oxygen bridges are directed towards the inside of the cavity produces a high electron density and gives some Lewis-base character.[3]

1.2.2 Inclusion Complexes and Kinetics

The CD cavity can accommodate a variety of organic guests,[9, 41-44] however, strong interactions are usually associated with hydrophobic molecules. The only requirement for inclusion of guests appears to be spatial and therefore the different cavity sizes allow α-CD to include benzene derivatives, for β-CD to include naphthalene and for γ-CD to include anthracene.[5,9]

Inclusion complex formation is usually associated with unfavourable entropy changes and favourable enthalpy changes.[4] The favourable enthalpy change is thought to be caused by: the Van der Waals interactions between the CD and its guest (London dispersion attraction and dipole-dipole interactions)[5], hydrogen bonding between the hydroxyl groups of the CD and the guest, high energy water molecules released upon complex formation, and strain energy being released in the macromolecular ring of the CD.[4]

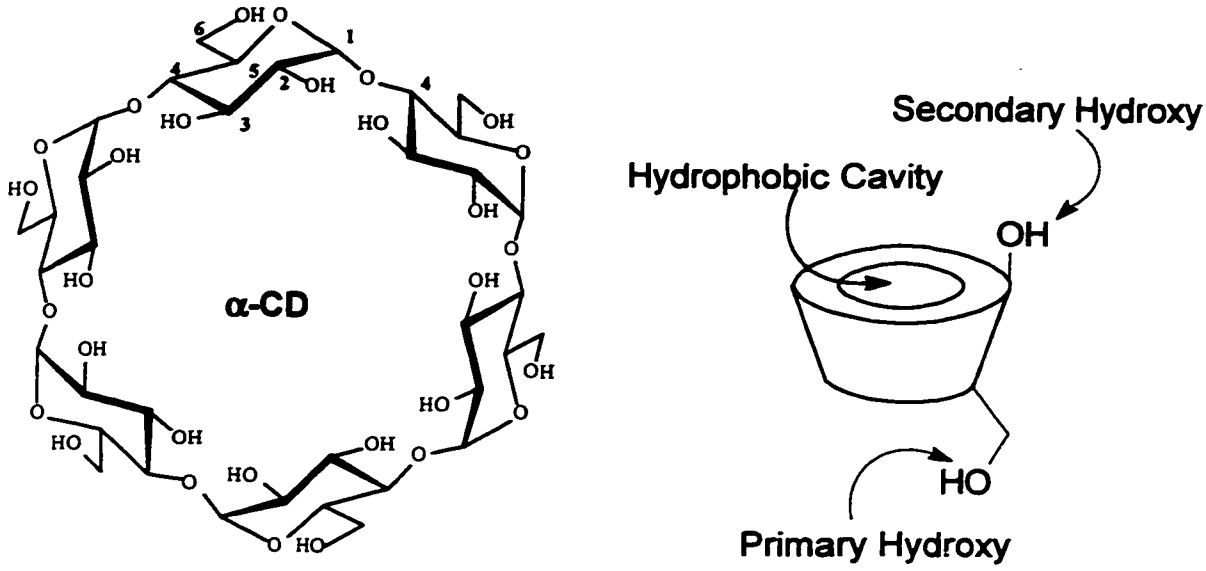

Scheme 1.3 Structure of an α-CD Molecule and a Schematic Representation of the Binding site of a CD Molecule.

The study of the complexes formed by CDs with their guests can be undertaken by various methods depending on the type of information sought. When essential information about factors involved in complexation are needed, dissociation constants are easily measured. The dissociation constant of a complex is an

equilibrium constant (K_S) for the dissociation of two or more molecules that form this complex.[8] K_S relates to the stability of the complex, [51] and from equation 1.0 the Gibbs free energy can be obtained.

$$\Delta G^\circ = -RT \ln K \qquad (1.0)$$

The stronger a guest binds to a host the lower the K_S value. As previously mentioned, this is because the binding energy is higher and usually results in a slower rate of dissociation.[6] Several factors influence the binding strength and hence the dissociation constant value. These factors were enumerated and explained in Section 1.1.

Some examples of K_S values for binding to β-CD are presented in Table 1.0. The larger the K_S value is the lesser interaction there is between the host and the guest. Note how the values depend on the guest size and shape.

Table 1.0 Dissociation Constants (K_S) of β-CD.Guest Complexes

Guest	K_S, mM	Reference
CH_3-CH_2-CH_2—OH *n*-propanol	216 ± 7	12
CH_3-CH_2-CH_2-CH_2—OH *n*-butanol	54.7 ± 4.2	12

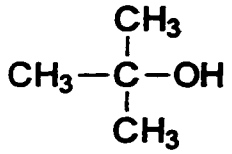

tert-butanol | 21.5 ± 0.4 | 12

$CH_3-(CH_2)_4-CH_2-OH$

n-hexanol | 4.00 ± 0.05 | 12

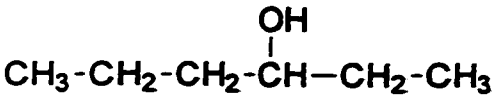

3-hexanol | 17.7 ± 0.27 | 14

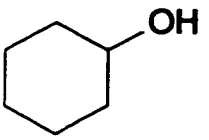

Cyclohexanol | 1.44 ± 0.14 | 12

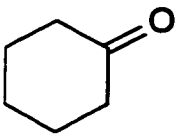

Cyclohexanone | 2.82 ± 0.05 | 12

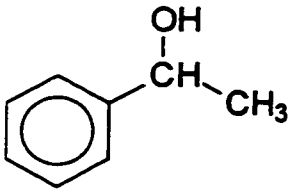

1-Phenylethanol | 9.54 ± 0.25 | 14

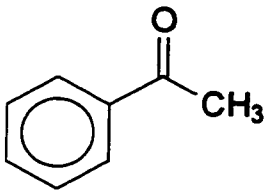

Acetophenone | 8.11 ± 0.55 | 14

One of the methods that we have employed to calculate dissociation constant values involves the use of "inhibition kinetics".[12-14] Using saturation kinetics several equations can be defined:

$$S \xrightarrow{k_u} P \qquad (1.1)$$

$$S + CD \underset{}{\overset{K_S}{\rightleftharpoons}} S.CD \xrightarrow{k_c} P \qquad (1.2)$$

$$K_S = \frac{[S]\,[CD]}{[S.CD]} \qquad (1.3)$$

$$k_{obs} = \frac{(k_u K_S + k_c [CD])}{(K_S + [CD])} \qquad (1.4)$$

The first equation (1.1) involves the conversion of the substrate (S) to the product (P) without the involvement of a "catalyst". The rate constant of the reaction is therefore written as k_u for "uncatalyzed". Equation (1.2) describes the conversion of S to P in the presence of CD. The substrate can form a 1:1 complex with CD (S.CD) and then be converted to P. The dissociation constant of this complex is expressed as K_S (equation 1.3). k_c represents the rate constant of the reaction from the S.CD complex to P (c is used for "catalyzed"). From equations (1.1, 1.2 and 1.3), equation (1.4) is derived, where k_{obs} is the observed (measurable) rate constant. Experiments can be carried out where only the [CD] is varied and k_{obs} is measured. Analysis of the results using equation (1.4) provides calculated values for the rate constant k_c and the dissociation constant K_S.

1.2.3 Effect of CDs on reactions

Depending on the reaction, CDs can have one of two effects. The first case is catalysis, which implies that with increasing [CD] k_{obs} will increase as seen in Figure 1.1. This is because the "uncatalyzed' rate constant (k_u) in equation (1.4) is smaller than the "catalyzed" rate constant (k_c). CDs have been known to catalyze a large number of reactions.[3-5,10] Catalysis of a reaction by CDs, or a catalyst, resides in their ability to lower the free energy of the transition state.[9] This can be done via non-covalent or covalent interactions. Non-covalent catalysis may involve one of two possible effects, microsolvent effect or conformational effect.[3,4] Covalent catalysis involves the formation of covalent intermediates.[3,4] The second case is retardation, where $k_c < k_u$. Therefore k_{obs} decreases with increasing [CD] (Figure 1.2).

1.3 Probe Reactions, Hydrolysis of TMOB and BDMA

Of the reactions that were found to be retarded by CDs, two were of particular interest, the hydrolysis of trimethyl orthobenzoate and the hydrolysis of benzaldehyde dimethyl acetal. Both reactions were well known and had previously been studied.[11-13] In their own right these reactions were interesting because they are relatively fast and their products are chromophores which made them suitable for stopped-flow experiments.

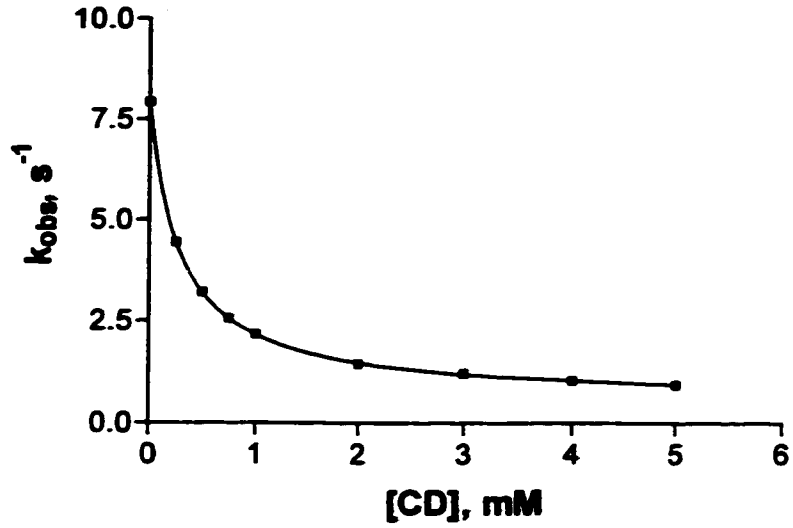

Figure 1.1 Catalysis of the Cleavage of m-Nitrophenyl Alkanoate by α-CD.[47]

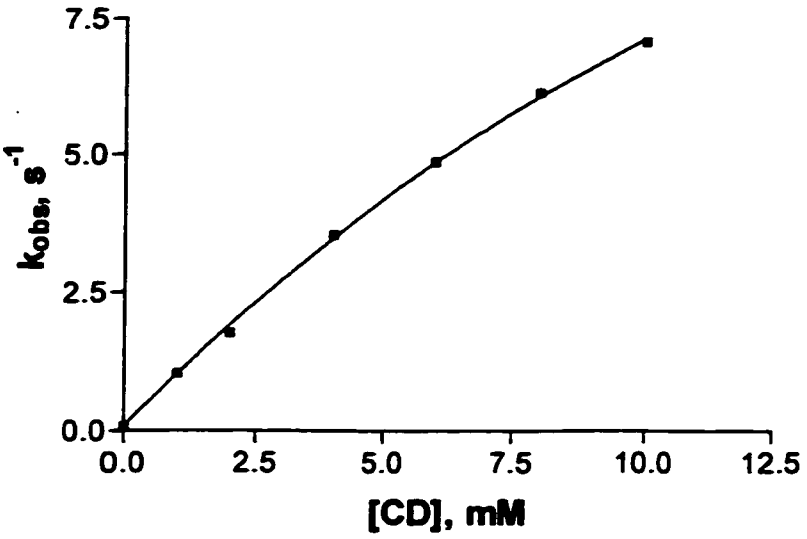

Figure 1.2 Retardation of the Hydrolysis of TMOB in 0.1 M HCl by β-CD.

In the case of acid catalyzed hydrolysis of TMOB, two major steps are involved:

$$PhC(OMe)_3 + H_2O \xrightarrow{H^+} PhC(OH)(OMe)_2 + MeOH \qquad (1.5)$$

$$PhC(OH)(OMe)_2 \xrightarrow[\text{or base}]{\text{acid}} PhC(O)OMe + MeOH \qquad (1.6)$$

Where the first step (1.5) involves general-acid catalysis and is rate-limiting.[11] Appearance of the product, methyl benzoate, can be monitored by measuring the absorbance increase at 228 nm.

The acid catalyzed hydrolysis of BDMA follows a similar course.

$$PhCH(OMe)_2 + H_2O \xrightarrow{H^+} PhC(OH)(OMe) + MeOH \qquad (1.7)$$

$$PhCH(OH)(OMe) \xrightarrow[\text{or base}]{\text{acid}} PhCHO + MeOH \qquad (1.8)$$

Step (1.7) is the acid catalysed conversion of the acetal to the hemiacetal, followed by step (1.8) where a molecule of methanol is eliminated by acid or base catalysis.[12] Benzaldehyde appearance can be monitored by measuring the absorbance increase at 252 nm.

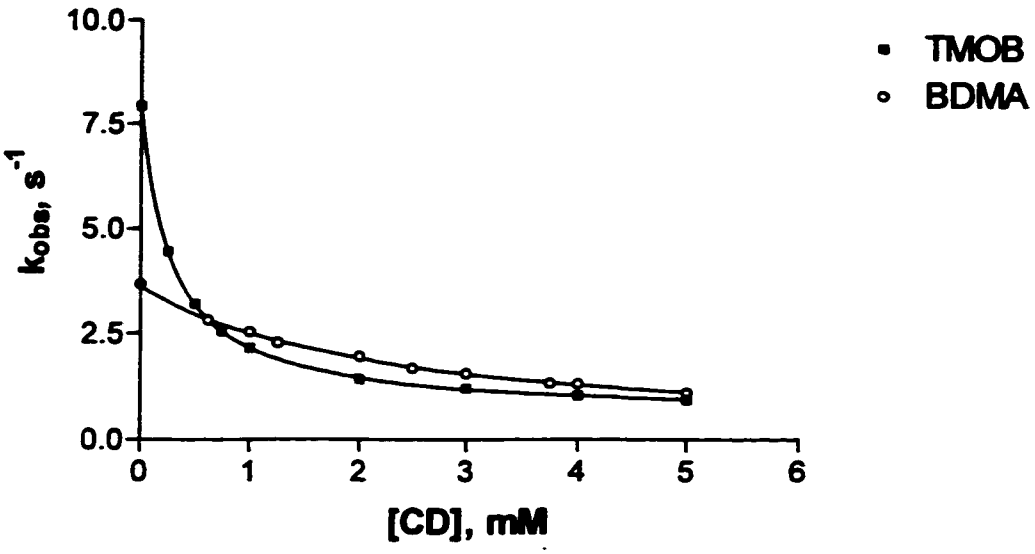

Figure 1.3 Retardation of the Hydrolysis of TMOB and BDMA in 0.1 M HCl by β-CD.

Discovery of the effect that β-CD has on these reactions[12,13] lead to the conclusion that they could be used as probe reactions. By making use of inhibition kinetics, and carrying several experiments under the same conditions with the exception of the [CD], which was varied (Figure 1.3), pertinent information (k_c and K_S) could be estimated. Analysis of the results yielded the parameters presented in Table 1.1

To exploit inhibition kinetics as probes, equations have to be elaborated. By adding an "inhibitor" or a guest, *i.e.* a molecule that binds to CD, to the reaction mixture, with increasing concentration, an increase in the observed rate of the reaction is expected. The guest would compete with the substrate for the CD, therefore increasing the amount of free substrate available for hydrolysis.

The guest can form a complex with the CD and the dissociation constant can be expressed as equation (2.0).

$$CD + I \underset{}{\overset{K_I}{\rightleftharpoons}} CD.I \qquad (1.9)$$

$$K_I = \frac{[CD]\,[I]}{[CD.I]} \qquad (2.0)$$

An estimation of the [CD] compared to the $[CD]_0$, is obtained as follows:

$$[CD]_0 = [CD] + [CD.I] \qquad (2.1)$$

$$[I]_0 = [I] + [CD.I] \qquad (2.2)$$

$$[I] = [I]_0 - ([CD]_0 - [CD]) \qquad (2.3)$$

$$\text{so, } K_I = \frac{[CD]\,([I]_0 - [CD]_0 + [CD])}{([CD]_0 - [CD])} \qquad (2.4)$$

The [CD] is estimated using equation (1.4) where [CD] may be isolated to yield:

$$[CD] = \frac{(k_{obs} - k_u)\,K_S}{(k_c - k_{obs})} \qquad (2.5)$$

All the parameters are known with the exception of K_I which can therefore be calculated.

Table 1.1 Constants for the Hydrolysis of Acetals in the Presence of Cyclodextrins.

Substrate	k_u, s^{-1}	K_S, mM	k_c, s^{-1}	k_c/k_u
α-CD				
TMOB[a]	8.14	17.3±0.9	4.81±0.06	0.59
BDMA[a,d]	3.70	46.5±3.1	0.589±0.119	0.16
ADMA[e]	8.00	49.3±1.6	3.52±0.08	0.44
BDEA[f]	1.01	23.4±0.3	0.0859±0.0048	0.0850
β-CD				
TMOB[a]	7.94	0.281±0.004	0.573±0.018	0.072
BDMA[a,b]	3.62±0.02	2.26±0.05	0[c]	0
ADMA[e]	8.02	0.247±0.006	0.0507±0.0296	0.0063
BDEA[f]	0.988	1.83±0.20	0.0407±0.0318	0.0412
γ-CD				
TMOB[a]	8.12	9.32±0.48	0.394±0.129	0.049
BDMA[a,g]	3.66	51.3±0.4	0[c]	0
ADMA[e]	7.93	12.6±0.3	0.397±0.073	0.050

[a] In 0.10 M HCl, at 25 °C. Values of k_u, K_S and k_c were obtained by non-linear fitting of equation (1.4).
[b] See ref. 12
[c] Value indistinguishable from zero.
[d] See ref. 48
[e] Acetophenone dimethyl acetal in 0.010 M HCl, at 25 °C. See ref. 46
[f] Benzaldehyde diethyl acetal in 0.1 M Chloroacetate buffer. See ref. 49
[g] See ref. 50

1.4 Alcohols as Guests

The use of inhibition kinetics to calculate the dissociation constants of different CD complexes was proven to yield satisfactory results,[12-14,45-49] particularly when alcohols were used as guests.[12,13] Table 1.2 illustrates the results obtained with TMOB and BDMA hydrolysis as probe reactions in determining the dissociation constant of alcohols to β-CD.

Comparing K_i values with literature values and values obtained with a different probe reaction demonstrated strong agreement.[12,13] The validity of this method established, a new goal could be undertaken: the study of the interactions of β-CD with sugars.

1.5 Sugars as guests

In previous years, several publications presented the interactions of CDs with sugars.[16-19] Surprisingly, the results of some groups seem to disagree strongly with the results of other groups. Due to their size and properties, it was believed that sugars would interact weakly with CDs. Hirsh *et al.* estimated with a blood glucose meter a dissociation constant (K_i) for {β-CD.D-glucose} complex of 2.38 mM.[16] In contrast, Hacket *et al.* determined by fluorometric competition titrations in water a K_i value of 1667 mM for the same complex.[17] From the conflicting results comes the interest to study the interaction of cycloheptaamylose, β-CD, with several sugars using a different method: kinetics measurements.

Table 1.2 β-CD host-guest dissociation constants, K_i (mM)

Guest	ADMA[a]	TMOB[b]	BDMA[c]	Lit.[d]	Lit.[e]
1-Propanol	184±7	171±7	216±7	241	269
2-Propanol	189±2	163±6	218±8	246	263
1-Butanol	42.4±4.7	45.1±2.7	54.7±4.2	56	60.3
1-Pentanol	12.8±0.3	11.2±0.6	15.3±0.1		15.9
			14.7±0.2		
1-Hexanol	4.07±0.18	3.76±0.12	4.00±0.05	4.4	4.57, 4.4
1-Heptanol	1.27±0.01	1.25±0.06	1.38±0.24		1.41
3-Hexanol	16.2±0.6	14.6±0.2	17.2±0.6	17.7	
tert-Butanol	20.3±1.0	18.4±1.4	21.5±0.4		20.9
Cyclohexanol	1.51±0.09	1.44±0.06	1.44±0.14	1.49	2.00
		1.32±0.03	1.47±0.23		1.40-2.00[f]

[a] Acetophenone dimethyl acetal, in 0.01 M HCl at 25 °C. Product increase monitored at 244 nm. See ref. 46

[b] From the effect of guests on the retardation of the hydrolysis of trimethyl orthobenzoate by CDs in 0.10 M aqueous HCl.[12]

[c] From the effect of guests on the retardation of the hydrolysis of benzaldehyde dimethyl acetal by CDs in 0.10 M aqueous HCl.[12]

[d] From displacement of a fluorescent probe, at pH 11.6 (0.2 M phosphate buffer).[14]

[e] Mainly ref. 15.

[f] Other literature values.[52]

2. Results & Discussion

2.1 Effects of guests

As seen in the introduction, β-CD retards the hydrolysis of TMOB and BDMA. By adding a guest that binds to β-CD, and that competes with the substrate for the CD, an *increase* in the observed rate should be observed. An increase in the k_{obs} is expected because binding of the guest will lower the amount of free CD available, increase the free substrate, resulting in faster hydrolysis. The dissociation constant for the {β-CD.guest} complex (K_I) can be estimated by exploiting the same methodology as in "inhibition kinetics". In this case, the reaction is slowed down instead of catalysed and the inhibitor (sugar) *increases* the observed rate. Equations 1.4 and 2.4 derived in the Introduction and the k_u, k_c and K_S values from Table 1.1 are needed to estimate the K_I values. The estimation is done by obtaining k_{obs} for a reaction including a guest (sugar) at several known initial concentrations. The K_I values estimated in this work are shown in Table 2.1.

Table 2.1 Dissociation constants for the {β-CD.guest} complexes

Guest	K_t, mM				
	Lit[a]	Lit[b]	TMOB	BDMA	ADMA[c]
Pentoses					
D-arabinose	1430	667	1060±80	1500±220	1070±45
L-arabinose	1430		949±90	1050±50	1230±54
D-2-deoxyribose	106		63±16	145±3	134±12
D-lyxose	233		394±24	456±21	404±11
D-ribose	189	159	209±16	252±11	210±8
D-xylose	1000	625	573±20	757±13	834±75
L-xylose			480±32	958±124	775±74
DL-xylose			427±66	1020±85	786±30
Hexoses					
D-fructose			1170±86	1800±90	1670±100
D-galactose		2000	3920±890	2960±300	3500±185
D-glucose		1670	2630±130	4720±400	5390±730
D-mannitol			3650±210	8720±2020	4250±260
D-mannose		1000	1460±190	2790±235	2540±180
L-rhamnose			503±76	1640±140	1190±58
D-sorbitol			1200±150	3420±180	4110±290
L-sorbose			665±46	829±76	969±27
Others					
β-D-lactose			2200±82	10400±1700	5550±1760
sucrose			2200±380	3190±290	6030±2060
D-glucosamine.HCl			813±48	847±27	1040±110

[a] Reference 18.
[b] Reference 17.
[c] Hydrolysis of acetophenone dimethyl acetal in 0.01 M HCl (monitored for acetophenone at 244 nm). Work performed by Samer Hussain.[46]

The "inhibition kinetic" method can only be used if the guest binds in the cavity of the CD. This is because the probe substrate is bound inside the CD cavity. The interior of the CD is relatively hydrophobic which prevents solvated protons from reaching the substrate and supresses its hydrolysis. If the guest interacts with the exterior of the β-CD, this will not be monitored. It is possible that the sugars associate outside of the cavity, a point that Hacket *et al.* have raised, [17] and that has been demonstrated by NMR to occur between protons on the outside the CD host cavity and those of cyclohexanecarboxylate in unpublished work by Gadre *et al.*, cited by Hacket *et al.* [17] If the sugars interact with the exterior of the β-CD cavity, the actual binding constant of the {sugar.β-CD} complex may be different than the estimated K_i value. As an example, if a sugar is bound on the exterior of the cavity is blocking the opening of the CD, then the substrate is "locked" in the CD cavity and cannot be hydrolysed. The rate of hydrolysis would be lower than if the sugar was bound in the CD cavity, leading to a lower estimated concentration of bound sugar, resulting in a larger dissociation constant for the {sugar.β-CD} complex. One cannot conclude that the sugars are actually interacting on the exterior of the CD cavity since there is a lack of proof, nevertheless, many indications suggest that they are. In fact this might explain the observed enhancement in solubility of the β-CD in the presence of glucose noticed by Hacket *et al.*[17]

The results obtained by Hirsch *et al.*[16] may reflect a similar ambiguity: their dissociation constants for {glucose.β-CD} are very small which implies strong binding, and the method they used only monitored the free glucose, it could not

differentiate between glucose interacting in the CD cavity or on the exterior of the CD cavity. If the glucose is binding to the exterior of the CD cavity, less free glucose will be detected, and a lower K_i values will be estimated. This could be a possible explanation for the estimated K_i value of 2.38 mM for {glucose.β-CD} complex. More over, Hirsch et al. found that the dissociation constants for the {glucose.α-CD} and {glucose.β-CD} complexes were indistinguishable within experimental error, which is not usually the case for large molecules like glucose. The α-CD cavity is of smaller diameter (0.6 nm) than β-CD (0.8 nm) and the general binding pattern is that β-CD can accommodate branched and cyclic compounds better, as seen in several publications and studies.[13,14a] If the glucose is binding to the exterior of the CD cavity, it is possible that the K_i values are relatively the same for α-CD and β-CD, if not, the dissociation constants are unlikely to be so similar.

The titration microcalorimetry used by de Namor et al.[19] is another technique that cannot distinguish between the sugar interacting with the exterior or the interior of the CD cavity. And the same thinking as for the Hirsch et al. values may apply here, since the K_i values reported by de Namor et al. are significantly lower than the K_i values by Hacket et al., Aoyama et al. or this work (see Figure 2.6). One has to keep in mind that at the moment, all this thinking is purely speculative and that further studies and experiments have to be performed in order to confirm or reject it.

The TMOB and BDMA values were obtained under the same acidic conditions and using the same sugar solutions, therefore comparing them is one way of determining if the estimated K_i values are reasonable. Figures 2.3 and 2.4

presents the correlation of the BDMA values with the ADMA (obtained in lower [HCl]) values as well as with the TMOB values. Figure 2.5 shows the correlation of the ADMA values with the TMOB values. The correlation coefficient values are shown in Table 2.2.

Table 2.2 Correlation coefficients for the comparison of the pK_I values estimated using different probe reactions

Correlation	Pentoses	Hexoses	Others
BDMA vs ADMA	0.977	0.880	0.885
BDMA vs TMOB	0.937	0.819	0.894
ADMA vs TMOB	0.949	0.855	0.965

In general, the values seem to agree, which is significant since most of the K_I values obtained were large (explained further). Within experimental error the results show appreciable constancy, the difference in the K_I values are most likely due to the distinct probe reactions. A low K_I value is estimated more precisely due to the strong binding: the effect of a guest is greater when it interacts strongly with its host, the increase in k_{obs} is larger therefore the range of the values used in the calculations is bigger, resulting in less error. The fact most sugars interact weakly with β-CD is a major source of error, as one can notice in Table 2.1, the lower K_I values have usually smaller relative error values. It is also important to note that the pentoses values agree more closely than the hexoses or the others sugars values,

which is further proof that estimation of a binding constant for weakly interacting host and guest is difficult. When comparing the estimated values with the literature values the correlation coefficient values obtained are presented in Table 2.3.

Table 2.3 Correlation coefficients for the comparison of the pK_i values estimated to the pK_i values from the literature

Correlation	**TMOB**	**BDMA**	**ADMA**
Aoyama[a]	0.929	0.963	0.983
Hacket[b]	0.978	0.932	0.954

[a] Reference 18.
[b] Reference 17.

Figure 2.1 shows the values from this work plotted against the Aoyama[18] values and Figure 2.2 shows the estimated K_i values compared to the Hacket[17] values. The K_i values obtained in our work tend to agree well with the literature values from these two publications, even though the methods used were very different. In contrast, when looking at Figure 2.6, one can obviously see that the $\Delta G°$ values, and therefore the K_i values, from de Namor *et al.* and Hirsch *et al.* do not correlate with our values. This may be due to the fact mentioned previously (sugars interacting with the exterior of the cavity) or the difference in the techniques used.

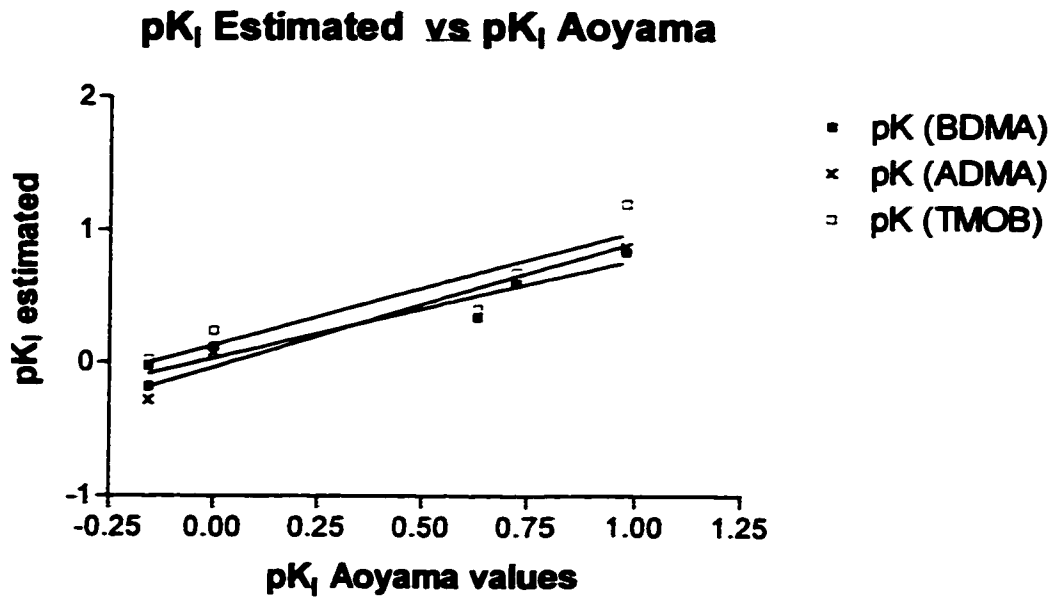

Figure 2.1 pK$_I$ estimated values from this work vs literature pK$_I$ values from Aoyama *et al.*.[18]

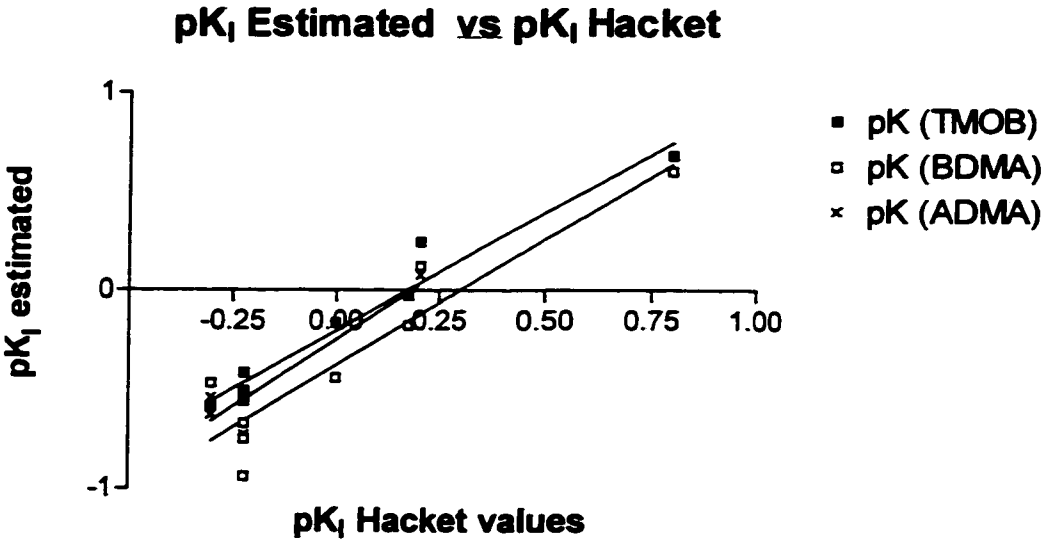

Figure 2.2 pK$_I$ estimated values from this work vs literature pK$_I$ values from Hacket *et al.*.[17]

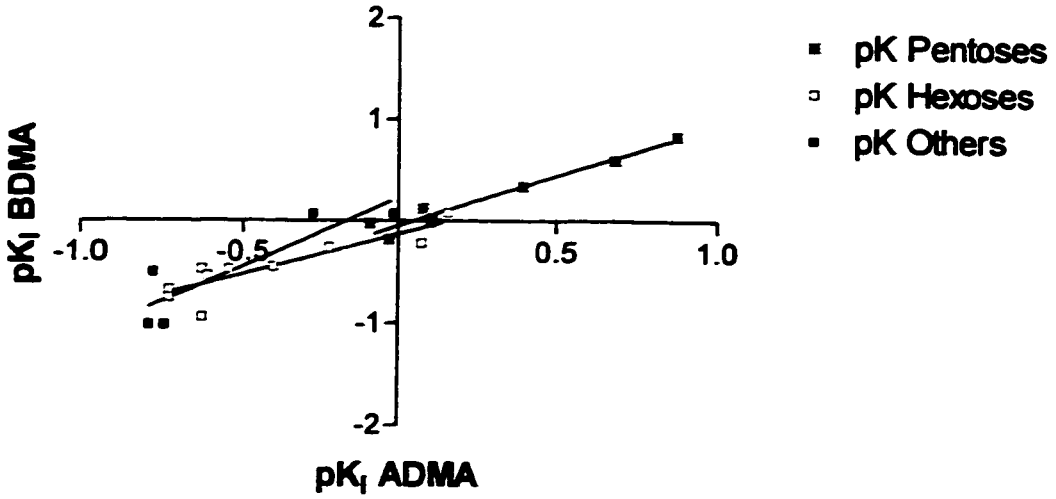

Figure 2.3 pK$_I$ estimated values from this work for benzaldehyde dimethyl acetal vs pK$_I$ estimated values for Acetophenone dimethyl acetal.

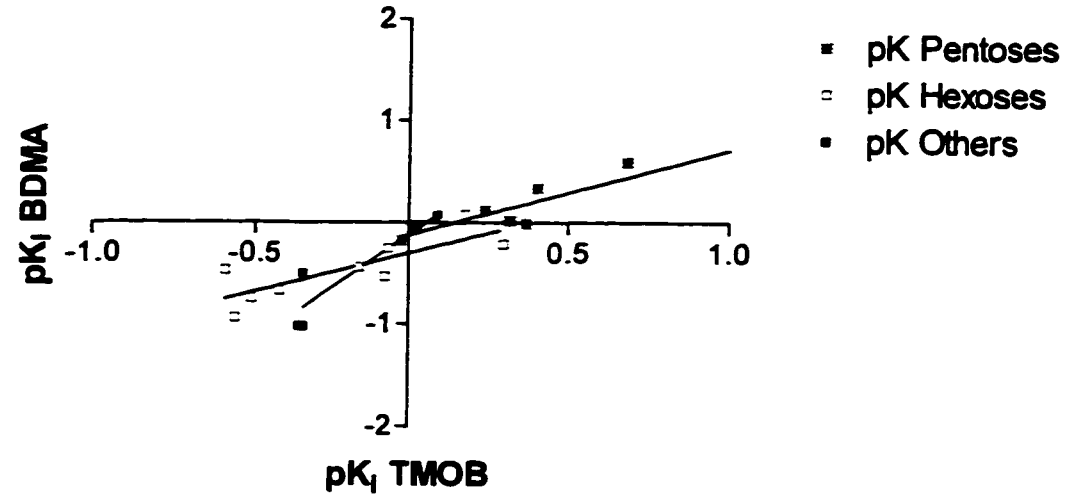

Figure 2.4 pK$_I$ estimated values from this work for benzaldehyde dimethyl acetal vs pK$_I$ estimated values from this work for Trimethyl orthobenzoate.

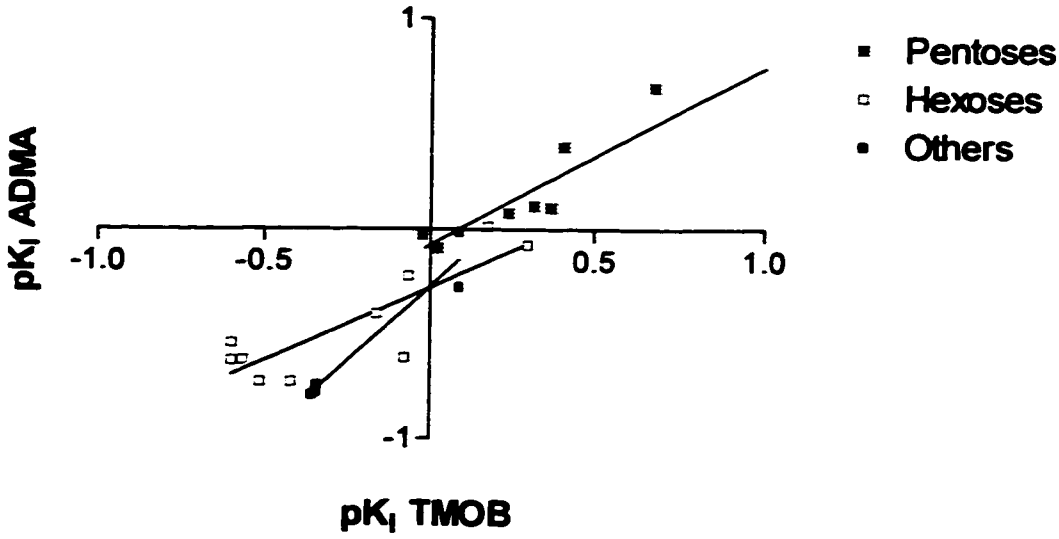

Figure 2.5 pK$_I$ estimated values for Acetophenone dimethyl acetal vs pK$_I$ estimated values from this work for Trimethyl orthobenzoate.

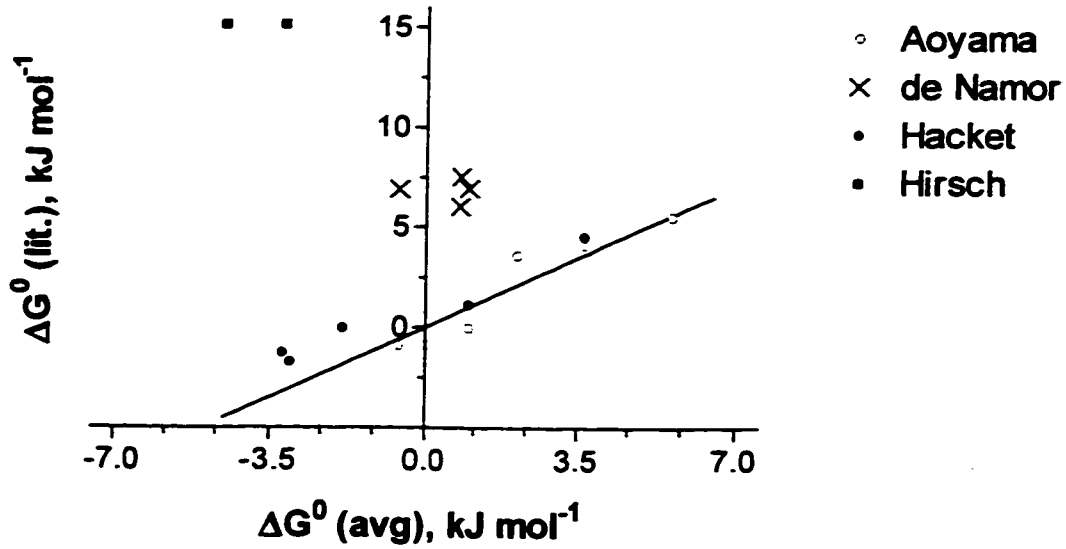

Figure 2.6 ΔG° values from the literature vs ΔG° averaged values of BDMA and TMOB from this work.

2.2 Sugars structure

The structure of most of the sugars used in this work are shown in Appendix A. The majority of them are found to be in the pyranose form in solution.[31-33] In general, there is an equilibrium between the α and β form of the sugars. At this point, the anomer or anomers present in solution and mutarotation is not the main concern. This is because mutarotation is promoted by acids and bases and temperature dependent, the rate of the reaction may double or triple every increment of 10 °C.[33] In this case, the reactions were carried at room temperature and at low acid concentration. The important factor is which cyclic form the sugars adopt. For some sugars, only one cyclic form is found, as an example, α-D-glucopyranose exhibits a simple mutarotation suggesting that only the α- and β-pyranoses exist in solution.[33] For other sugars, both cyclic forms are present, and in the D-ribose case, no chair conformation is preferred ($^1C_4$ or $^4C_1$).[33] Which makes it difficult to determine what type of structure is interacting with β-CD.

In general, the pentoses bind more tightly to β-CD than the hexoses. Figures 2.7, 2.8, 2.9 and 2.10 present the k_{obs} vs the sugar concentrations for the pentoses and hexoses. By looking at those graphics one can see the effect that adding sugars has. The tighter the sugar binds, the more effect can be seen, as an example in figures 2.7 and 2.8, 2-deoxy-D-ribose (2-deoxy-D-*erythro*-pentose)[34] demonstrates the larger increase in k_{obs} with increasing concentration. Using TMOB as a probe reaction, the dissociation complex of 2-deoxy-D-ribose was estimated to be 63 ± 16 mM. In the case of BDMA, it was estimated to be 145 ± 3 mM. Which explains why a larger effect for 2-deoxy-D-ribose is seen in Figure 2.7 than in Figure

2.8.

The lowest dissociation constant was found to be for the complex {2-deoxy-D-ribose.β-CD}. The reason for this most likely stands in the structure of this sugar. 2-deoxy-D-ribose is the most important 2-deoxy-aldose since it is a component of deoxyribonucleic acids (DNA). The form and conformation of this sugar in solution was not studied and therefore is not known with certainty. In DNA, 2-deoxy-D-ribose exists in the furanose form,[34] so this might be the case in solution. The sugar could also be found in an acyclic form. Both these forms could explain why this sugar binds the most tightly, since no other sugars adopt them in solution (with the exception of the alcohols).

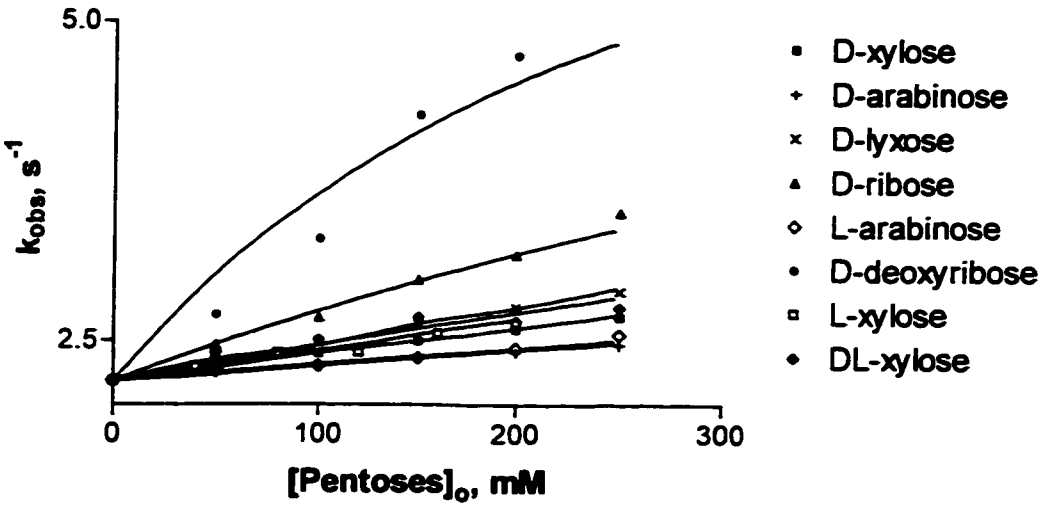

Figure 2.7 k_{obs} scaled vs [Pentoses]$_0$ for the hydrolysis of TMOB in the presence of 1 mM of β-CD.

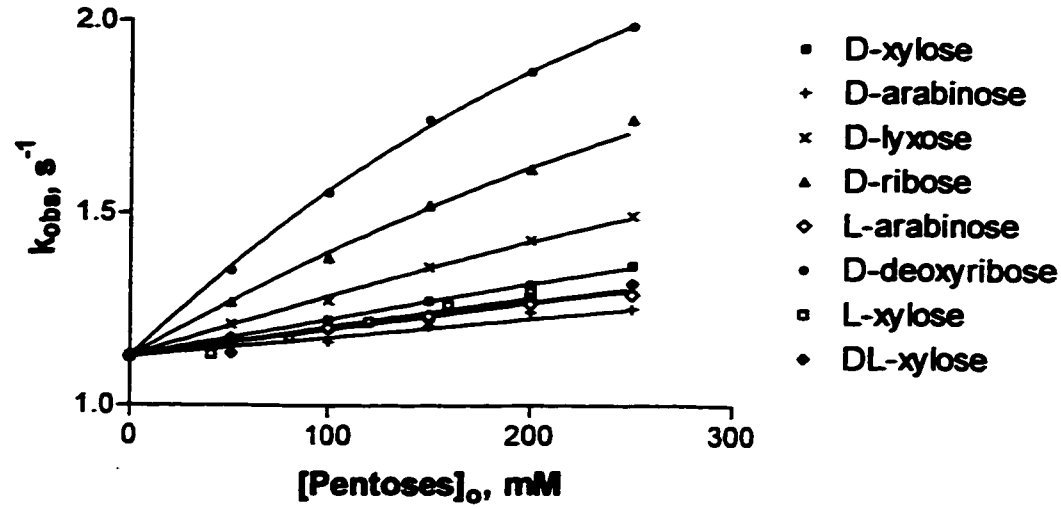

Figure 2.8 k_{obs} scaled vs [Pentoses]$_0$ for the hydrolysis of BDMA in the presence of 5 mM of β-CD.

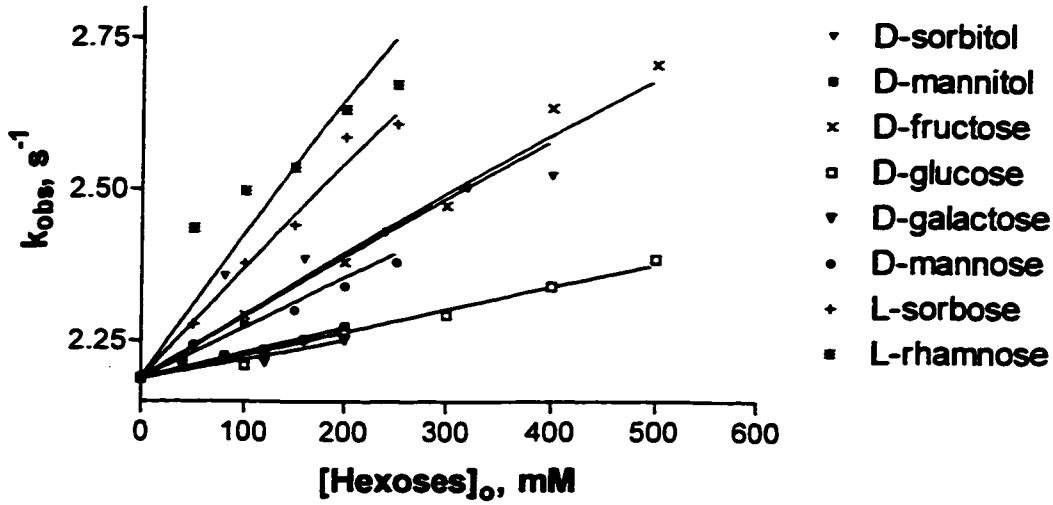

Figure 2.9 k_{obs} scaled vs [Hexoses]$_0$ for the hydrolysis of TMOB in the presence of 1 mM of β-CD.

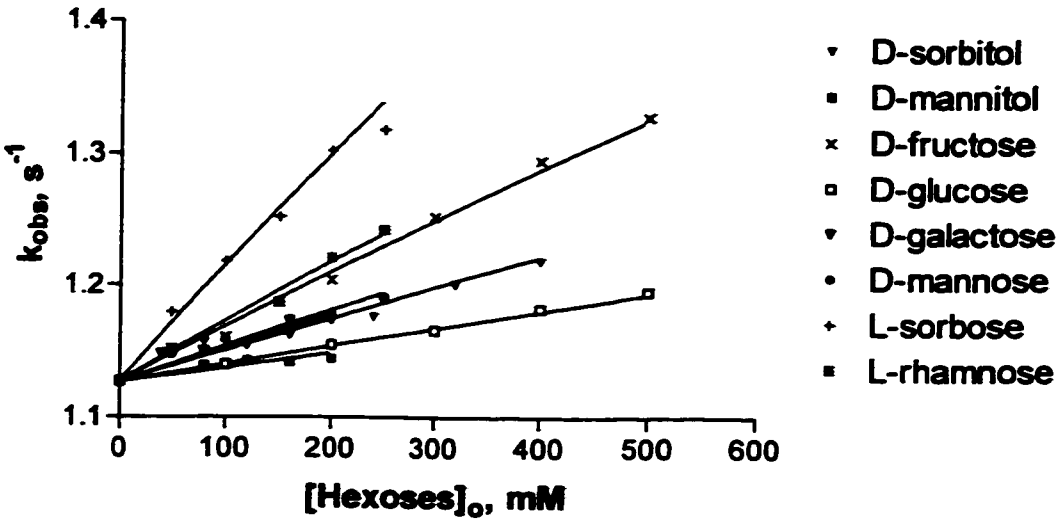

Figure 2.10 k_{obs} scaled vs [Hexoses]$_0$ for the hydrolysis of BDMA in the presence of 5 mM of β-CD.

The xyloses all show relatively the same effect with both probe reactions. The configuration of these sugars does not seem to affect their binding to β-CD. In the case of the arabinoses one can see the same pattern: the configuration does not seem to affect the binding. By contrast, the conformation seems to be slightly more important with respect to the binding. D-arabinose adopts the $^1C_4$ conformation in solution and the D-xylose adopts the $^4C_1$ in solution. Even though both those sugars have three hydroxyl groups in the equatorial position and one in the axial position, their dissociation constants differ only by approximately a factor of 2. The anomer also seems to be a factor in the case of D-arabinose and D-xylose. The different anomers indicate the "steric arrangement, with respect to the conformational disposition."[35] This explains why both sugars have the same number of axial and equatorial groups while they have different conformations.

α-D-Lyxose has a $^4C_1$ preferred conformation and two axial hydroxyl groups

and two equatorial hydroxy groups. α-D-xylose adopts the same conformation but differ in the number of axial hydroxyl groups since those two sugars are 4-epimers. The effect of adding those two sugars are similar when using TMOB, but differ slightly when using BDMA. This may be caused by the different probe reactions.

α-D-Ribose does not have a preferred conformation in solution[32], and it can be found in the pyranose form (76-80%) and the furanose form (24-20%). Therefore several structures of ribose will be in solution, this may explain why it binds the tightest after 2-deoxy-D-ribose. D-ribose is the true epimer (2-epimer) of D-arabinose[34], but those epimers do not have similar binding constants (they differ by a factor of approximately 5).

The hexoses show less of an effect on the kinetics and this is reflected in the dissociation constants estimated. The hexoses are larger molecules and might not be as well accommodated by the β-CD as the pentoses. D-mannitol is one of the six-carbon carbohydrates that did not bind tightly to the cyclodextrin. This compound is found in an acyclic form in solution and was thought of having easy access to β-CD cavity. The other alcohol studied, D-sorbitol (D-glucitol), did bind more tightly to β-CD. This sugar is also found in an acyclic form in solution but with a bent-chain arrangement,[34] due to an unfavourable 1,3 interaction between two oxygen atoms. The bent-chain arrangement may facilitate the accommodation of D-sorbitol by β-CD, resulting in a lower dissociation constant.

D-glucose and D-galactose are 4-epimers and behave in the same manner for both probe reactions. D-glucose and D-mannose are true epimers and differ in their effect with TMOB and BDMA. The position of the hydroxyl group on C-2 seems

an important one in the binding of the sugars to β-CD since all of the true epimers studied were found to behave differently and have large variation in their binding constants.

The sugars that have the lowest dissociation constant are L-rhamnose and L-sorbose. L-rhamnose is a deoxy sugar (6-deoxy-L-mannose) and L-sorbose is a ketose (D-*xylo*-hexulose) with a carbonyl group on C-2. 2-Deoxy-D-ribose was the pentose with the lowest dissociation constant and here again we have a deoxy sugar for the hexoses. More over, both 2-deoxy-D-ribose and L-rhamnose contain carbonyl groups (not on C-2). It seems that the sugars that posses a carbonyl group are better accommodated by β-CD.

α-D-Fructose is an hexose that can be found both in the pyranose form (68.4-76.0%) and the furanose form (31.6-24%). α-D-Ribose is a pentose that is also found in both forms, and it is interesting to see that they both bind the tightest after the deoxy sugars (L-rhamnose and 2-deoxy-D-ribose). Again, this may be explained by the different structures found in solution. It is important to note that fructose (D-*arabino*-hexulose) is a ketose with a carbonyl group at carbon atom no. 2.

Figures 2.11 and 2.12 present k_{obs} vs the sugars concentrations for various monosaccharides, both pentoses and hexoses. When sugars adopt the pyranose form, some of the pentoses and hexoses have the same structure, that differs only by the R group on carbon 5. It is interesting to compare them and see if they behave in the same manner.

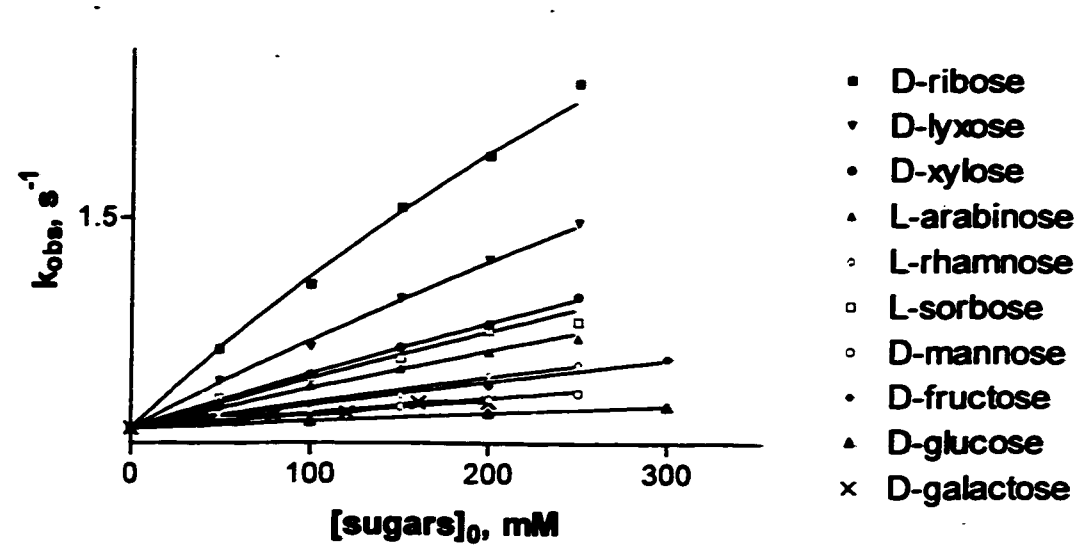

Figure 2.11 k_{obs} scaled vs [sugars]$_0$ for the hydrolysis of TMOB in the presence of 1 mM of β-CD.

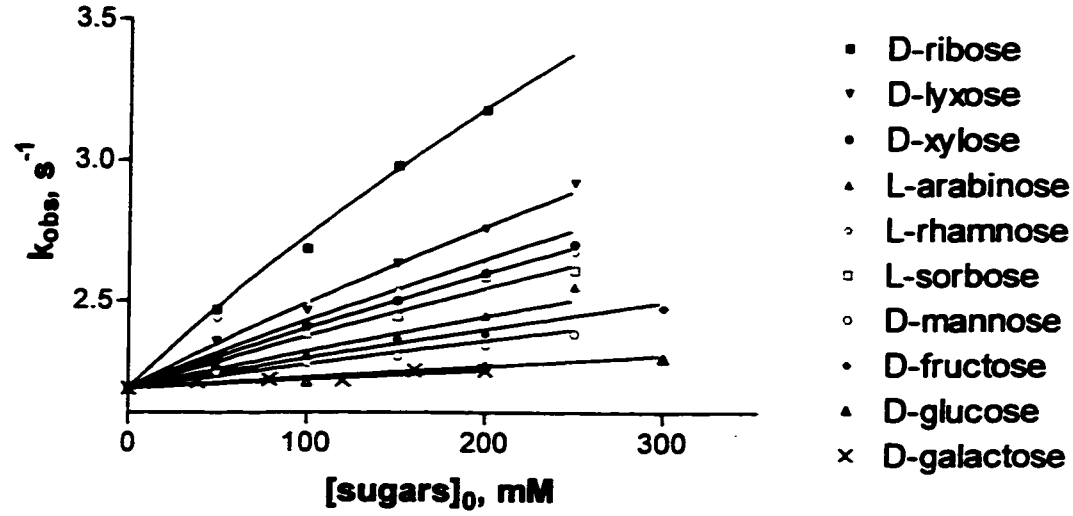

Figure 2.12 k_{obs} scaled vs [sugars]$_0$ for the hydrolysis of BDMA in the presence of 5 mM of β-CD.

The first two sugars to be compared are D-glucose and D-xylose. They adopt the same conformation, but do not have the same anomer *i.e.* that the hydroxyl group on C-1 is in the α position for D-xylose and in the β position for D-glucose. By looking at Figures 2.11 and 2.12 one can see that D-glucose does not bind as tightly to β-CD as D-xylose. Two factors could be involved: The R group on C-5 and/or the position of the hydroxyl group on C-1. α-D-lyxose and β-D-mannose are similar to α-D-xylose and β-D-glucose, they both have the same conformation and differ by their anomer. Here again, the α-aldopentose binds more tightly to β-CD than the β-aldohexose. Now, β-D-galactose and α-L-arabinose do not have the same conformation or anomer. These two aldoses also have different dissociation constants.

The results in Table 2.1 are clear, the pentoses have lower dissociation constants than the hexoses, therefore the R group on C-5 is a major factor in the binding of the carbohydrates to β-CD, which was also observed by Aoyama *et al.*[17] It also becomes evident that the α anomers bind more tightly to β-CD than the β anomers. This leads to the conclusion that both the R group on C-5 and the position of the hydroxyl group on the C-1 are important factors involved in the interaction of β-CD to monosaccharides.

D-glucosamine hydrochloride has the same structure as D-glucose, with the exception of having an NH_2 group on C-2. The glucosamine has a lower dissociation constant than D-glucose. This agrees well with the previous statement that "the position of the hydroxyl group on C-2 seems an important one in the binding of the sugars to β-CD since all of the true epimers studied were found to behave

differently and have large variation in their binding constants."

Two oligosaccharides were studied, β-D-lactose and sucrose. It is interesting to note that both these sugars have, within experimental error, approximately the same dissociation constants as D-glucose. For sucrose, this might indicate that not all the sugar is accommodated in the β-CD cavity and that either the glucose or fructose part of the molecule binds to the cyclodextrin. The same could apply to β-D-lactose, where either the D-galactose or D-glucose part of the molecule could interact with the β-CD. Since the values for those two sugars are similar, it is most likely the glucose part of the molecule that binds to the cyclodextrin.

Since the K_i values from the {β-CD.oligosaccharides} complexes are so large (over a 1000 mM) they indicate that very little interactions are occurring between the β-CD and the sugars. A value over a 1000 mM is almost meaningless and hardly reproducible. It is possible that the values for β-D-lactose and D-glucose are similar because of a large deviation rather than an indication of what part of the molecule is involved in binding.

3. Conclusion

The rate of hydrolysis of trimethyl orthobenzoate and benzaldehyde dimethyl acetal were confirmed to be slowed down by β-CD. By exploiting the saturation type kinetics involved and using "inhibition kinetics", the dissociation constants (K_i) for several {β-CD.sugar} complexes were estimated. These K_i values were found to correlate well with the values obtained using the acidic hydrolysis of acetophenone dimethyl acetal as a probe reaction.[46] It was also demonstrated that the results obtained in this work agreed tolerably with the results of Hacket et al.[17] and of Aoyama et al.,[18] but there are strong disagreements between our results and those of de Namor et al.[19] and of Hirsch et al.[16] These conflicting results do not seem to indicate flaws in the technique used. It could possibly mean that the sugars are binding with the exterior of the cyclodextrin, as well as in the cavity. The viability of the acidic hydrolysis of TMOB and BDMA as probe reactions in estimating dissociation constants for the binding of guests to CDs had been established before[12,13] and this work provides further evidence to confirm this statement. This work did not provide astonishing results as it was expected that β-CD would interact only slightly with sugars. Pentoses were found to bind modestly to β-CD (K_i = 100 - 1000 mM) and hexoses hardly bind at all (K_i > 500 mM).

4. Experimental

4.1 Materials

β-Cyclodextrin was purchased from Wacker Chemie (Munich, Germany). Trimethyl orthobenzoate (TMOB), benzaldehyde dimethyl acetal (BDMA) and all the sugars were obtained from Aldrich Chemical Co. Standard HCl solutions were purchased from A & C Chemicals (Montréal).

4.2 Kinetic Experiments

The kinetic experiments were carried out by using a single beam stopped-flow spectrophotometer by Applied Photophysics model SX17MV. In the stopped-flow apparatus the mixing is 1:1 and so the concentrations of the two solutions before and after mixing differ by a factor of 2. The observation cell was kept at 25.0 ± 0.1 °C. The sugar solutions were prepared in 0.10 M HCl. A concentration after mixing of 1 mM of β-CD was used for the hydrolysis of TMOB. The concentration of TMOB and BDMA after mixing was 5 mM (50 µl of 0.1 M solution in 50 ml flask before mixing) The concentration after mixing of β-CD for the hydrolysis of BDMA was 5 mM.

The hydrolysis of TMOB in 0.10 M HCl was monitored for changes in absorbance at 228 nm for the appearance of the product, methyl benzoate. The hydrolysis of BDMA under the same conditions was monitored for changes in absorbance at 252 nm for the appearance of its product, benzaldehyde.

4.3 Calculation of Rate Constants

Using the instrument manufacturer's software, the observed rate constants (k_{obs}) were calculated by fitting the absorbance increase with a single exponential function. The absorbance traces were composed of 400 points. For the purpose of this work, the first 15 points were not taken into account when calculating k_{obs}, to allow for the small induction period.[12] Each recorded k_{obs} value is derived from the average of 5 - 10 absorbance traces. Absorbance traces extended over 7 half-lives for the hydrolysis of TMOB and 8 half-lives for the hydrolysis of BDMA.

4.4 Calculation of Dissociation Constants

The calculation of K_I values was carried out following the procedure explained in the Introduction. In a spread sheet (see Scheme 4.1) the [CD] was estimated using equation 2.5:

$$[CD] = \frac{(k_{obs} - k_u) K_S}{(k_c - k_{obs})} \qquad (2.5)$$

and this was used to estimate K_I, through equation 2.4. A dissociation constant was calculated for each concentration of guest or "inhibitor" added. The K_I values were then averaged and a graph of k_{obs} vs k_{calcd} was plotted to verify the linear relationship. A sample calculation is shown in Scheme 4.1, overleaf.

The k_{obs} values are entered in the second column of the spread sheet, and these values are scaled according to the k_{calc}. The calculated rate constant (k_{calc}) was determined using the known parameters presented in Table 1.1. In Scheme 4.1, k_{calc} was calculated for the hydrolysis of TMOB in 0.10 M HCl in the presence of 1 mM of β-CD in solution and was found to be 2.188 s^{-1}. Different factors may

influence the k_{obs} obtained for a $[CD]_0$ = 1 mM and $[guest]_0$ = 0 mM: the precise [CD] and the [HCl]. By scaling the observed rate constants to a calculated rate constant comparison by graphic representation is facilitated, since the initial point for all inhibition analysis are the same.

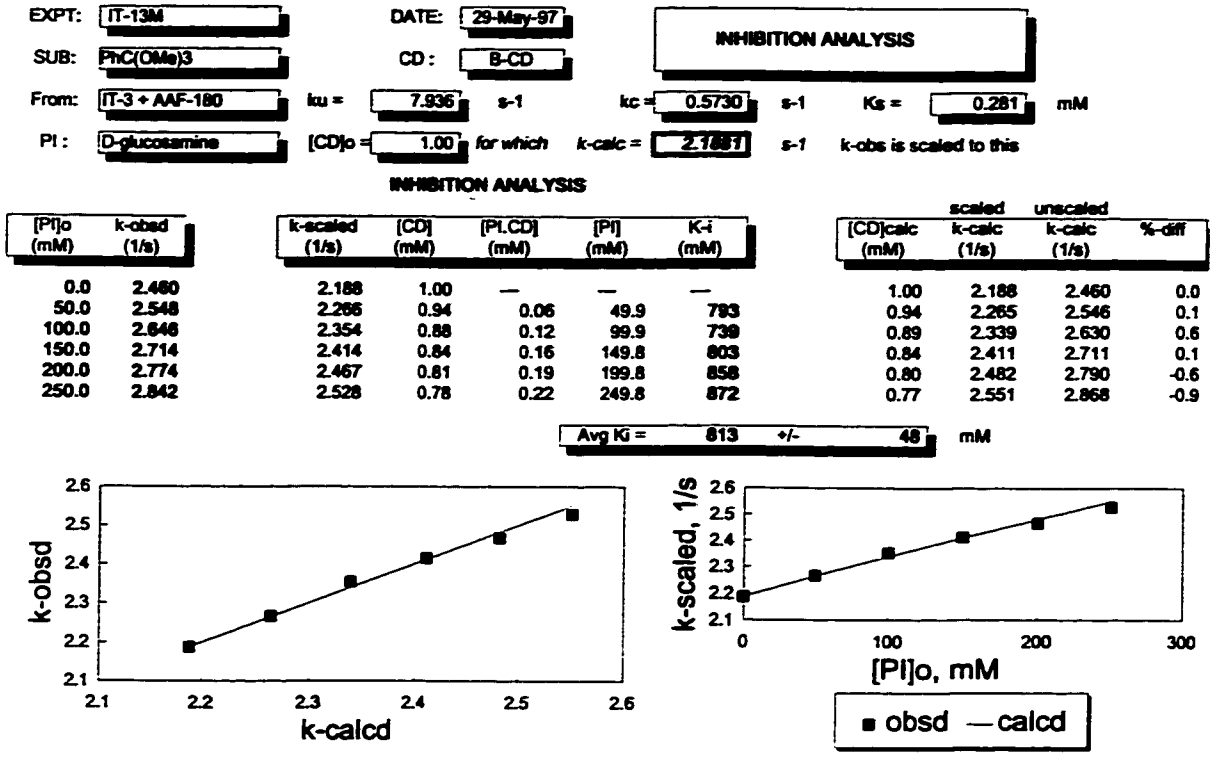

Scheme 4.1 Calculation of the dissociation constant of D-glucosamine to β-CD using a Lotus 1-2-3 spread sheet.

PART II

The Bromination of Pyrimidine Derivatives

5. Introduction

5.1 Pyrimidine Structure and Properties

Pyrimidine derivatives are important heterocycles since they are essential components of nucleic acids as well as some coenzymes and drugs.[20] Pyrimidine, itself, is composed of a six-membered aromatic ring containing two nitrogen atoms, as seen in Scheme 5.1. The pyrimidine molecule is symmetrical with two planes of symmetry, with one plane and axis of symmetry going through carbons 2 and 5, which makes positions on carbons 4 and 6 equivalent, as well as positions 1 and 3 equivalent. Yielding an overall C_{2V} symmetry.

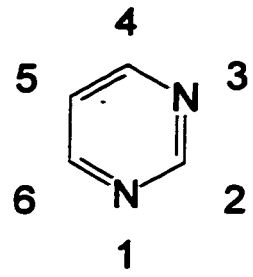

Scheme 5.1 Structure of Pyrimidine Molecule

The nitrogens are powerful electron-withdrawing atoms resulting in electron-deficient positions 2, 4, and 6.[21] Their separate effects are reinforced because the nitrogen atoms are meta to each other.[21] The reactivity of substituent groups found in positions 2,4 and 6 will reflect the electron deficiency. Therefore, if a halogen atom is found in one of these positions, the halogen would be easily attacked by a

nucleophile.

The 5-position is much less electron-deficient due to the general inductive effect.[21] Consequently, electrophiles would attack at this point. Nitration, nitrosation, halogenation may easily be carried at this position.

When electron-releasing substituents are introduced, the pyrimidine reacts more as an aromatic ring because the π-electrons are restored. This facilitates electrophilic reactions at the 5-position. Some of these substituents are hydroxy and amino groups. As seen in Scheme 5.2, pyrimidines with these substituents in the 2,4 and 6 positions may be in equilibrium with their tautomeric forms. As an example, 2-aminopyrimidine will be tautomeric with its 2-imino form. Of course, the equilibrium will lie towards the more energetically favoured structure, and in the case of 2-aminopyrimidine, Brown and coworkers. found that in solution the major tautomeric form is the amino form.[22]

Amino

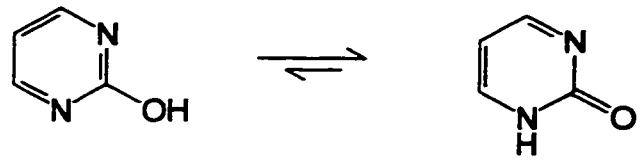

Hydroxy

Scheme 5.2 Equilibrium between Tautomeric forms of 2-AP *i.e.* the Amino and the Imino form and between the Hydroxy and the Ketone form of Pyrimidone.

5.1.1 Bromination of Pyrimidine Derivatives

5.1.1.1 Bromination of 2-Aminopyrimidine

The bromination of 2-aminopyrimidine (2-AP) has been largely studied through the years,[21-25] and it involves two major steps. First a fast step where addition of water and attack by bromine occur. The second step is slow elimination of water to yield the 5-bromo product. Further investigation into this reaction provided key information about the intermediate. This intermediate was isolated and observed by NMR by Banerjee,[24] who also had observed similar intermediates for the bromination of pyrimidone and uracil derivatives. Barbieri et al. had observed analogous intermediates in the bromination of pyrimidine sulphonamides in methanol solution.[26]

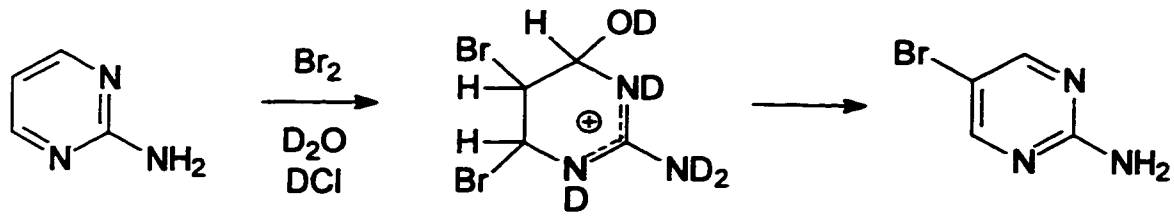

2-aminopyrimidine intermediate 5-bromo product

Scheme 5.3 Bromination of 2-AP in D_2O to observe the intermediate by NMR spectroscopy.

Following the observation of the intermediate in the bromination of 2-AP, an interesting question arises, how is this intermediate formed? Does it first involve the

attack of bromine then followed by addition of water or the inverse? This question was addressed by an undergraduate student in a CHEM 450 research project and thesis in 1980 but with no concrete conclusion.[25]

5.1.1.2 Bromination of 1,2-dihydro-2-imino-1-methylpyrimidine

The addition of bromine to 1,2-dihydro-2-imino-1-methylpyrimidine was studied in 1980, here again, a similar intermediate was isolated and observed by NMR.[25] In this case, can the same mechanism as for 2-AP by applied? If it can, do all the pyrimidine derivatives react with bromine in the same manner? More derivatives need to be studied.

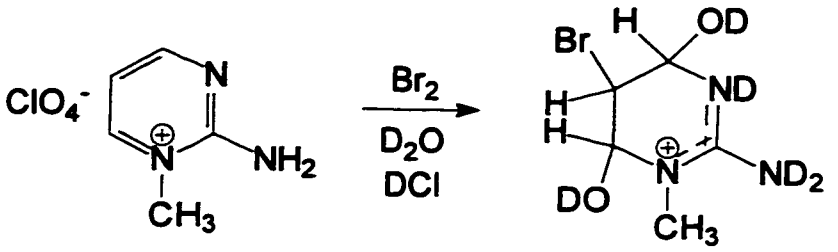

Scheme 5.4 The Bromination of M2A in D_2O to observe a similar intermediate by NMR spectroscopy.

5.1.1.3 Bromination of 2-Amino-4,6-dimethylpyrimidine

The literature contains very little information about the bromination of 2-amino-4,6-dimethylpyrimidine (2-ADP). The articles usually involve product studies.

Studying the bromination of 2-ADP could give insights about the mechanism involved, furthermore, it could be compared with other pyrimidine derivatives.

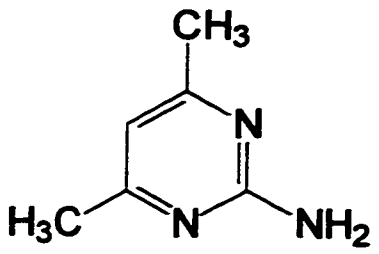

Scheme 5.5 Structure of 2-Amino-4,6-dimethylpyrimidine.

5.2 Pyridine Structure and Properties

The broad interest in pyridine and its derivatives has produced a lot of literature.[27] Pyridine is similar to pyrimidine, but it only contains one nitrogen atom. The molecule is relatively flat with bond angles close to 120°. The nitrogen atom is sp^2 hybridized and will contribute one π electron to the aromatic sextet. The other π electrons are provided by the carbon atoms.

Since the nitrogen atom is electron withdrawing it will have some negative charge. Partial positive charges are found at the 2,4 and 6 positions, creating an overall charge distribution of negative for the nitrogen atom and positive for the ring (Scheme 5.6). The properties of pyridine are parallel to benzene,[27] but with differences due to the presence of the nitrogen atom. The electronegative nitrogen

causes the pyridine to be more polar than benzene. Electrophilic substitution reactions can occur but with more difficulty than with benzene, and primarily at positions 3 and 5.

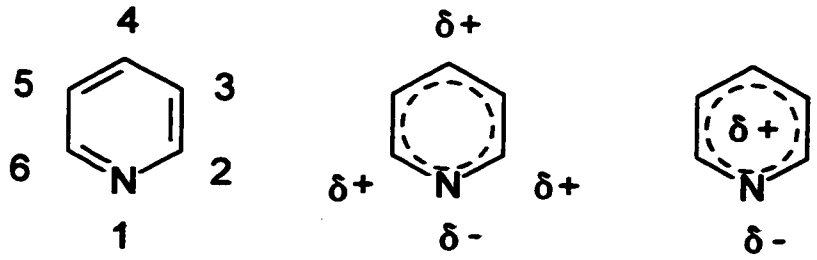

Scheme 5.6 The structure of Pyridine and the partial and overall charge distribution.

Electron-donating groups are ortho and para directing groups. Therefore, if a substituent is at the 2 position it further activates position 3 and 5 for electrophilic attack.

5.2.1 Bromination of Pyridine Derivatives

5.2.1.1 Bromination of 2-Aminopyridine

From the literature, it is known that the bromination of 2-aminopyridine (2-APy) yields a mixture of products. With excess bromine, the major products are 3,5-dibromo and 5-bromo-2-aminopyridine. To a lesser extent, the 3-bromo derivative is obtained. Occasionally, one gets 6-bromo and 3,5,6-tribromo derivatives.[27-29]

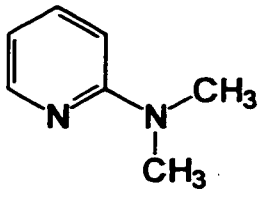

Scheme 5.7 The bromination of 2-Aminopyridine.

No study on the mechanisms involved have been undertaken. The interest in this type of study is for comparative reasons.

5.2.1.2 Bromination of 2-Dimethylaminopyridine

In the case of the bromination of 2-dimethylaminopyridine (2-DAPy), the literature states that with a limiting amount of bromine a mixture of the mono (5-bromo-2-dimethyl aminopyridine and dibromo (3,5-dibromo-2-dimethylaminopyridine) derivatives is obtained.[30]

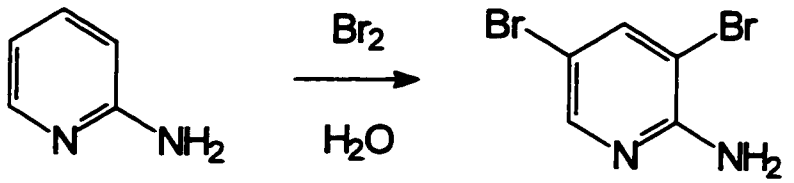

Scheme 5.8 The structure of 2-dimethylaminopyridine.

5.3 Aniline Structure and Properties

Aniline is an important compound in organic chemistry, not only for its chemical and physical properties, but for its historical background. In 1856, Henry Perkin oxidized impure aniline with potassium dichromate, yielding a purple pigment, which gave him the idea of using it as a dye. Following this discovery, Perkin resigned his post with Hoffman and created his own chemical company. To produce his dye on a large-scale he had to elaborate a method for preparing aniline, the early beginnings of organic synthesis and of the synthetic dye industry.[20]

Aniline is a benzene molecule with an amino substituent. It is less basic than simple alkylamines, because the electron lone-pair of the nitrogen atom is delocalized by orbital overlap with the π electron system of the aromatic ring and therefore less available for bonding.[2]

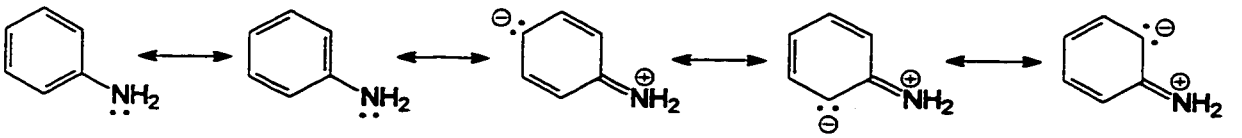

Scheme 5.9 Resonance structures of Aniline.

The protonation of the amino group of aniline is less favoured, because the resonance stabilization present in aniline is lost, due to the fact that only two principal resonance structures are possible for the arylammonium ion:

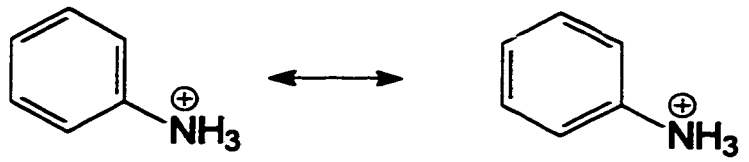

Scheme 5.10 Resonance structures of an arylammonium ion.

Substituents which decrease the reactivity of aromatics towards electrophilic attack also decrease the basicity of anilines. As an example, the pK_a of aniline is equal to 4.58 and that of the *p*-bromoaniline is equal to 3.86.[20] The basicity is affected by deactivating groups (electron-withdrawing groups) because they make the aromatic ring electron-poor. If the amino group is protonated, a deactivating substituent will decrease the stability of the positively charged ion, yielding a smaller ΔG° for protonation and a lower pK_a.

5.3.1 Bromination of Aniline

It is known that the bromination of aniline takes place rapidly and yields the 2,4,6-tribrominated product. The amino group being so strongly activating, and ortho- and para- directing, it is hard to stop at the monosubstituted product.[20]

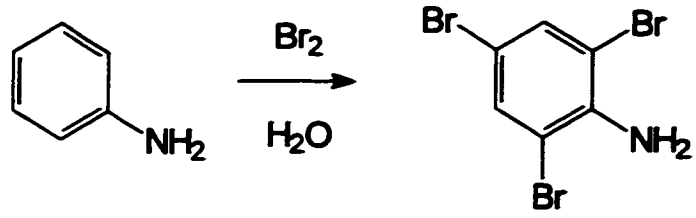

Scheme 5.11 The bromination of Aniline.

5.3.2 Bromination of *N,N*-Dimethylaniline

Similarly, the bromination of N,N,-dimethylaniline is rapid and with excess bromine the tribromo aniline is obtained.

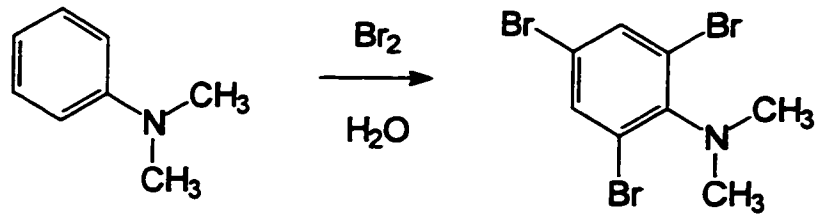

Scheme 5.12 The bromination of N,N-dimethyl aniline.

For the purposes of comparison with that of aminopyrimidines and aminopyridines, the study of the bromination of aniline and its derivative was considered important.

5.4 Simple Kinetics

To further understand the reaction of bromine with the aminopyrimidines, aminopyridines and anilines previously mentioned, kinetic equations can be derived.

These equations relate to the rate of the reaction and express the dependance of the rate on different factors such as the concentration. The kinetic equations can help resolve the mechanism puzzle.

Bromination is usually carried out under acidic conditions and the substrate can be found in the protonated or unprotonated form. Assuming that the bromine only attacks the unprotonated form, equation 2.7 would represent the reaction equation where S is the substrate, P is the product, K_a is the equilibrium constant between the protonated and unprotonated form of the substrate (equation 3.0) and k_2 is the second order rate constant for the bromination of the substrate. From the type of traces obtained, it can be established that the rate of the reaction will be equal to the disappearance of bromine, as shown in equation (2.8a). Since the disappearance of bromine is what is measured, k_2^{obs} is used for the observable second order rate constant. The rate of the reaction should also be equal to that required by the scheme (eq. 2.7) of the reaction as seen in equation (2.8b).

$$SH^+ \underset{H^+}{\overset{K_a}{\rightleftharpoons}} S + Br_2 \xrightarrow{k_2} P \qquad (2.7)$$

$$\text{rate} = -\frac{d[Br_2]}{dt} = k_2^{obs}\,[S]_0\,[Br_2] \qquad (2.8a)$$

$$\text{rate} = k_2\,[S]\,[Br_2] \qquad (2.8b)$$

$$k_2^{obs} = \frac{k_2\,[S]}{[S]_0} \qquad (2.9)$$

Knowing that both equations (2.8a) and (2.8b) are equal, one may isolate k_2^{obs} and obtain equation (2.9). Where [S] and $[S]_0$ differ due to the protonation of some

substrate. The substrate concentration may be substituted using equation (3.0) to yield equation (3.1).

$$K_a = \frac{[S][H^+]}{[SH^+]} \qquad (3.0)$$

$$k_2^{obs} = \frac{k_2 K_a}{(K_a + [H^+])} \qquad (3.1)$$

A low pH, *i.e.* at a pH lower than the pK_a value, equation 3.1 may be simplified to equation (3.2). The logarithmic version of this equation is shown in (3.3).

$$k_2^{obs} = \frac{k_2 K_a}{[H^+]} \qquad (3.2)$$

$$\log k_2^{obs} = \log k_2 K_a + pH \qquad (3.3)$$

A plot of $\log k_2^{obs}$ vs pH should yield a linear graphic where the intercept is equal to the $\log k_2$. This situation is applicable to the following substrates, where the pH of the experiments was always much lower than the pK_a values of the protonated form of each substrate: 2-APy, 2-DAPy, 2-ADP, aniline and *N,N*-dimethylaniline.

6. Results & Discussion

6.1 Bromination of Aniline

As seen in the Introduction, equation 3.3 can be used to express pH dependence of the the second order rate constant k_2. The requirement of this equation is that a slope of approximately 1 is obtained when log k_2^{obs} is plotted against pH. The pH rate profiles obtained for aniline and *N,N*-dimethylaniline (Figure 6.1) meet the requirements of equation 3.3 and the calculated results are tabulated in Table 6.1.

$$\log k_2^{obs} = \log k_2 K_a + pH \qquad (3.3)$$

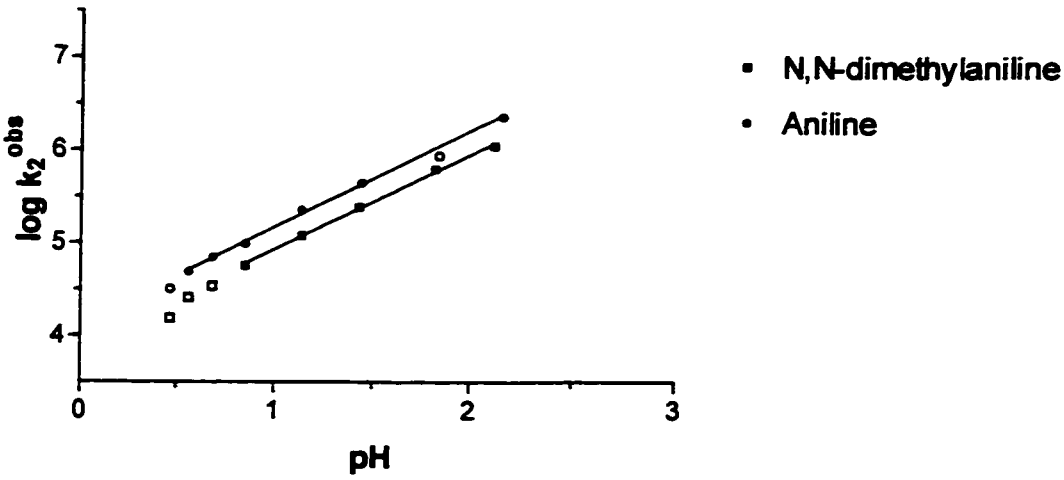

Figure 6.1 pH rate profile for the Bromination of *N,N*-dimethylaniline and aniline. The points with open symbols (□ and ○) were excluded from the calculations. This is mostly due to the high ionic strength at low pH.

Table 6.1 Bromination Parameters

	N,N-dimethylaniline[a]	Aniline[a]
pK_a	5.07[b]	4.58[b]
Slope	1.02 ± 0.03	1.04 ±0.02
log $k_2 K_a$	3.91 ± 0.04	4.13 ± 0.02
k_2	9.62 x 10^8 M^{-1} s^{-1}	5.11 x 10^8 M^{-1} s^{-1}
k_2^{app}	3.46 x 10^8 M^{-1} s^{-1}	1.84 x 10^8 M^{-1} s^{-1}
log k_2^{app}	8.54	8.27
r	0.999	0.999

[a] For an ionic strength of 0.1 M.
[b] Reference 38

The value k_2^{app} is the k_2 value before any corrections for the tribromide ion has been made in Table 6.1. The reason for estimating this value is that a value for *N,N*-dimethylaniline was available from the literature. Bell and Ramsden determined an apparent second-order rate constant of 3.16 x 10^8 M^{-1} s^{-1} for an ionic strength of 0.05 M,[36] whereas, the value for this work is 3.46 x 10^8 M^{-1} s^{-1} for an ionic strength of 0.10 M. These values are the same within experimental error, given the different ionic strengths. The simple linear relationship between the log of k_2^{obs} and pH leads to the conclusion that direct bromine attack on the unprotonated substrates is involved.

Aniline was expected to be less reactive towards bromine than *N,N*-

dimethylaniline. This is because aniline is less basic than N,N-dimethylaniline as stated in the Introduction. The effect of two methyl groups on the nitrogen atom is moderate, and k_2 was expected to be slightly higher for *N,N*-dimethylaniline. In order to compare the value obtained for aniline with the literature, a Hammett plot, Figure 6.2, was constructed using the values for substituted anilines taken from Katritzky *et al.*[37]

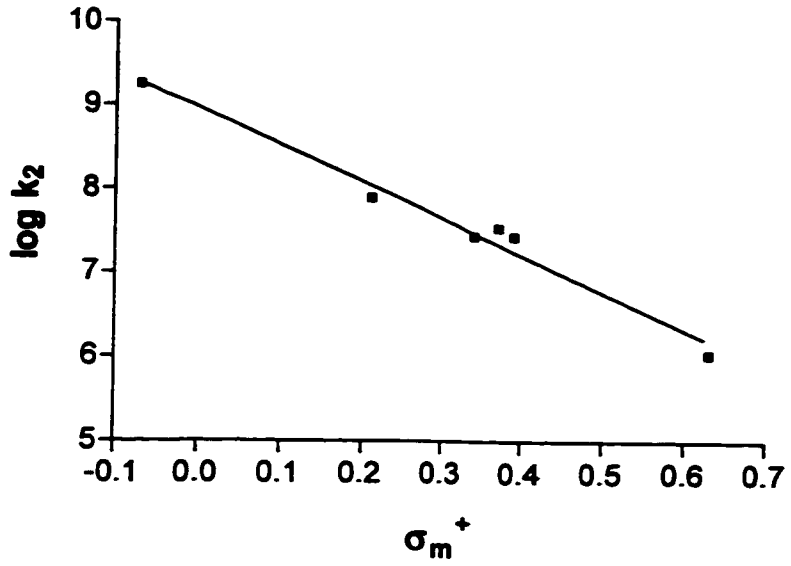

Figure 6.2 Hammett plot for the bromination of *p*-substituted anilines.[37] Substituents: F, Br, Cl, Me, NHAc, NH_3^+.

From the Hammett equation[54b] (3.4), the rate constant for the unsubstituted compound can be estimated.

$$\log k = \log k_0 + \rho\sigma \qquad (3.4)$$

In this equation ρ is the reaction constant and σ depends only on the substituent. From the plot of log k_2 vs σ_m^+, the intercept is equal to log k_2 for the unsubstituted aniline.

The results from this plot are shown in Table 6.2.

Table 6.2 Hammett Equation Parameters for aniline[a]

	Aniline
r	0.989
Slope (ρ)	-4.40 ± 0.33
log k_2	8.97 ± 0.13
k_2	9.33×10^8 M^{-1} s^{-1}

[a] From the literature data[37] in Figure 6.1.

There seems to be a discrepancy between the value of 9×10^8 M^{-1} s^{-1}, estimated from the Hammett plot, and the value of 5×10^8 M^{-1} s^{-1} measured in this work. This may have arisen because the literature results[37] were obtained in fairly strong acid and had to be extrapolated to aqueous solution.

6.2 Bromination of Aminopyridine

In the case of the pyridines, similar pH rate profiles were obtained, as seen in Figure 6.3. To compare the values of k_2 obtained in this work for the aminopyridines (Table 6.3), to earlier results. Two Hammett plots were constructed from the values for six derivatives studied by Katritzky *et al.*[37], these plots gave the parameters presented in Table 6.4, according to which the values of k_2 for 2-APy

and 2-DAPy should be 2 x 10^7 M^{-1} s^{-1} and 2 x 10^8 M^{-1} s^{-1}, whereas our measured values are 9.4 x 10^6 M^{-1} s^{-1} and 1.5 x 10^8 M^{-1} s^{-1} respectively.

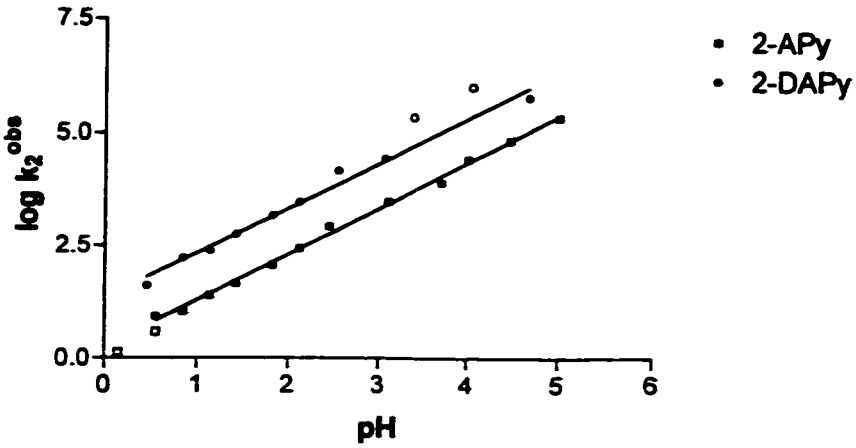

Figure 6.3 pH rate profile for the bromination of 2-aminopyridine and 2-dimethyl-aminopyridine. The points with open symbols (□ and ○) were excluded from the calculations.

Table 6.3 Bromination Parameters

	2-Aminopyridine[a]	2-Dimethylaminopyridine[a]
pK_a	6.71[b]	6.83[c]
Slope	1.02 ± 0.02	0.989 ± 0.044
$\log k_2 K_a$	0.261 ± 0.054	1.34 ± 0.10
k_2	9.35 x 10^6 $M^{-1}s^{-1}$	1.48 x 10^8 $M^{-1}s^{-1}$
$\log k_2$	6.97	8.17
r	0.998	0.993

[a] For an ionic strength of 0.1 M.
[b] Reference 38
[c] This work

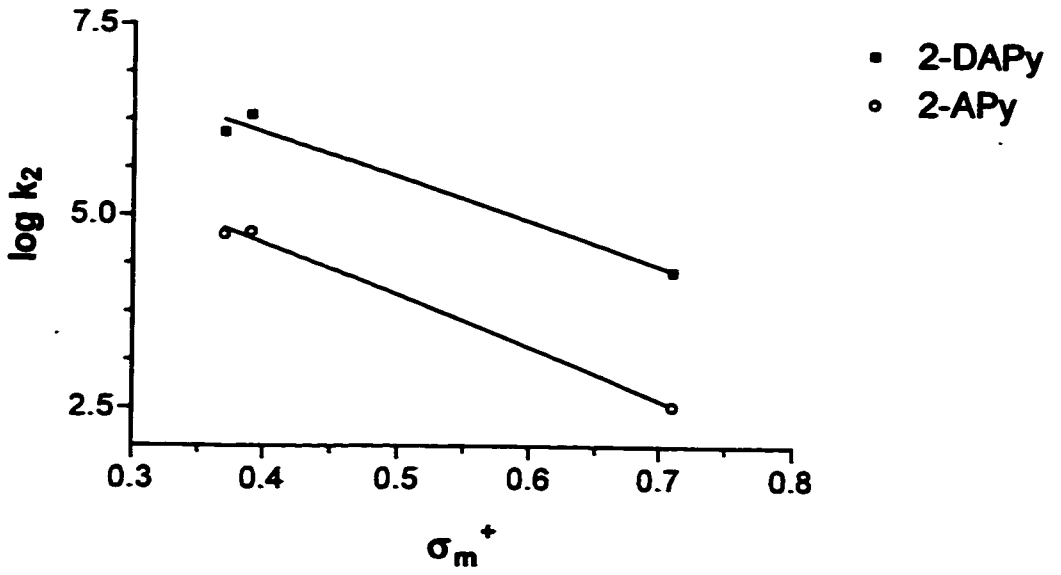

Figure 6.4 Hammett plot for the bromination of monosubstituted 2-Aminopyridine and 2-Dimethylaminopyridine at 20°C. Substituents: Br, Cl, NO_2.

Table 6.4 Hammett Equation Parameters for 2-APy and 2-DAPy[a]

	2-Aminopyridine	2-Dimethylaminopyridine
r	0.998	0.989
Slope (ρ)	-6.78 ± 0.43	-5.80 ± 0.88
log k_2	7.35 ± 0.22	8.40 ± 0.45
k_2	2.24 x 10^7 M^{-1} s^{-1}	2.51 x 10^8 M^{-1} s^{-1}

[a] From the data[37] in Figure 6.4.

The major source of the discrepancy for 2-APy is probably due to the limited number of points in the Hammett plot. Only three data points were available, and

so any slight deviation in the slope may result in a large variation in the y intercept (log k_2) value. It is interesting to note that the ratios of the second order rate constants (2-DAPy/2-APy) are quite similar. The ratio for our work is 15.8 whereas the ratio for the values estimated from the literature is 11.2.

The object of studying aniline, 2-aminopyridine (2-APy), and their N,N-dimethyl derivatives, was to observe the effect of an aza-nitrogen (=N-) in a benzene ring. From our value of k_2 for aniline and 2-APy, and the ρ^+ of -4.4 obtained by Katritzky et al.[37], we estimate a value of

$$\sigma_m^+ = \log (9.35 \times 10^6) - \log (5.11 \times 10^8)/-4.4 = 0.4$$

Assuming the effects of two aza-nitrogens in a ring are additive, then for bromine attack on 2-aminopyrimidine:

$$\log k_2 = \log (5.11 \times 10^8) - 4.4 (2 \times 0.4) = 5.19$$

And so an estimate of k_2 is 1.5×10^5 M^{-1} s^{-1}.

Alternatively, we can use a value of $\sigma_m^+ \approx 0.55$ for aza-nitrogen, derived earlier by Katritzky's group.[53] Using this value and the same ρ^+ gives an estimated k_2 of 7.4×10^3 M^{-1} s^{-1}. So, we expected 2-aminopyrimidine (2-AP) to react with bromine with a rate constant in the vicinity of 7400 to 150000 M^{-1} s^{-1}. As shown in the next section, we actually found a value of 2.5×10^4 M^{-1} s^{-1}, which is within the range mentioned above.

In a similar way, we can estimate a value of k_2 to be expected for bromine attack on 2-amino-4,6-dimethylpyrimidine (2-ADP). Proceeding as above, and using $\sigma_o^+ = \sigma_p^+ = -0.31$[54a],

$$\log k_2 = 8.71 - 4.4 (2 \times 0.55 + 2(-0.31)) = 6.60$$

and $k_2 \approx 4 \times 10^6\ M^{-1}\ s^{-1}$, which is very close to the value actually recorded in the next section.

6.3 Bromination of 2-Aminopyridimidine (2-AP)

Before we discuss the results obtained for the bromination of 2-AP, let us briefly look at the bromination of 2-amino-4,6-dimethylpyrimidine (2-ADP). No literature values are available for this particular compound. Since the studies of aniline derivatives and aminopyridine derivatives yielded satisfactory results, the assumption is that the results obtained for 2-ADP are also satisfactory. The kinetic parameters are presented in Table 6.5.

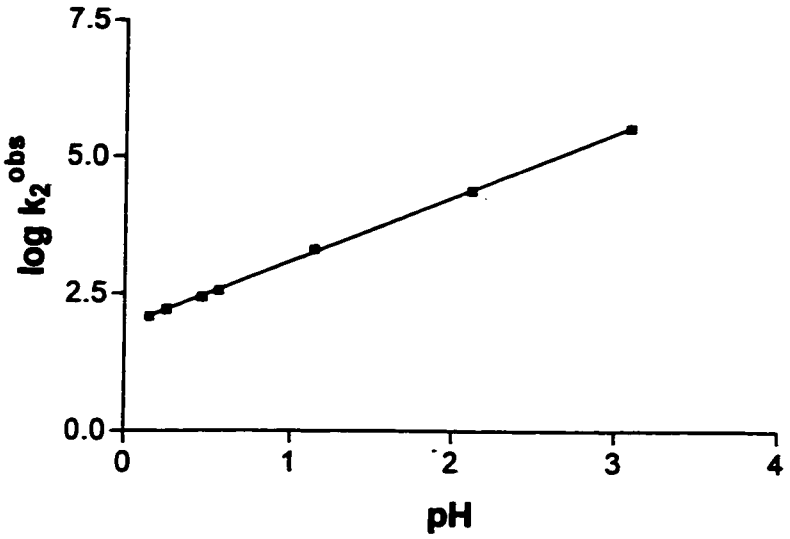

Figure 6.5 pH rate profile for the bromination of 2-amino-4,6-dimethylpyrimidine.

Table 6.5 Bromination Parameters

	2-Amino-4,6-dimethylpyrimidine[a]
pK_a	4.85[b]
Slope	1.17 ± 0.01
$\log k_2 K_a$	1.92 ± 0.01
k_2	5.87×10^6 M^{-1} s^{-1}
$\log k_2$	6.77
r	0.999

[a] For an ionic strength of 0.1 M.
[b] Reference 38

The value of $k_2 = 5.9 \times 10^6$ M^{-1} s^{-1} in Table 6.5 is very close to that estimated above (4×10^6 M^{-1} s^{-1}). Accordingly, it is concluded that 2-ADP reacts simply by direct attack of bromine on its free base form.

The pH rate profile of 2-aminopyrimidine is not straightforward, as seen in Figure 6.6. In fact, the "s" type curve indicates that more than one mechanism is involved.

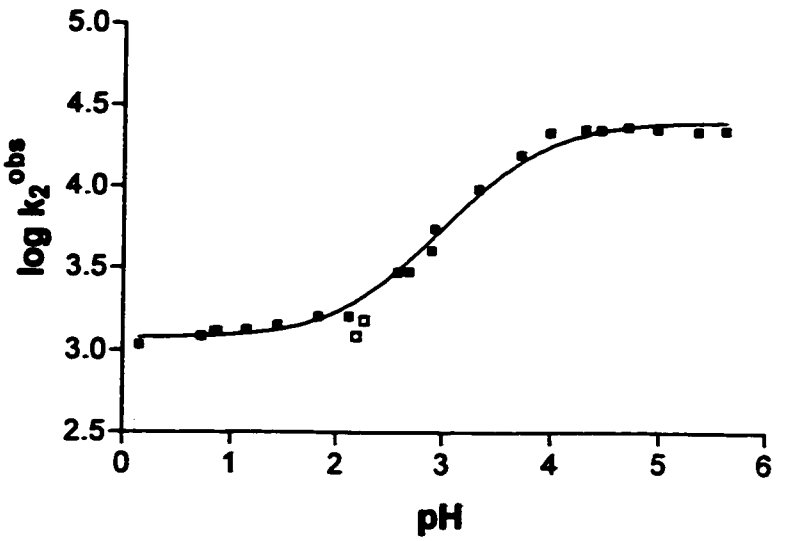

Figure 6.6 pH rate profile for the bromination of 2-aminopyrimidine.

At low pH (0 - 2) one mechanism is involved and at higher pH (2.5 - 6) another is taking part. Thinking in terms of kinetics, one can derive an equation which would correspond to the curve in Figure 6.6. Using this equation, the pK_a of 2-AP could be estimated.

In order to derive a kinetic equation, one must consider which species are reacting. The reactions were carried out under acidic conditions, therefore both the protonated and unprotonated forms of the substrate are present in solution. If the bromine can react with both forms, with k_2 as the rate constant for the bromine reacting with the protonated form and k_2' for the bromine reacting with the unprotonated form (Scheme 6.1), then, equation 3.5 can be derived.

$$k_2^{obs} = \frac{(k_2[H^+] + k_2' K_a)}{(K_a + [H^+])} \qquad (3.5)$$

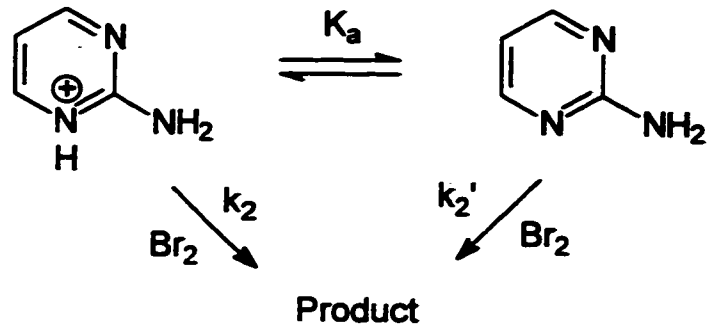

Scheme 6.1 Reaction of both forms of 2-AP with bromine in acidic solution.

The results obtained by fitting this equation are shown in Table 6.6. Note, in particular, that a pK_a of 3.66 was estimated, whereas the literature pK_a for 2-AP is 3.54 at 20 °C.[38] The agreement between these two values is obvious and it is an indication that the equation derived is appropriate, at least in part. Confirmation is also brought about by the fact that the data points are lying close to the curve.

Table 6.6 Bromination Parameters

	2-Aminopyrimidine[a]
pK_a	3.66 ± 0.05
k_2	1200 ± 60 M^{-1} s^{-1}
k_2'	25200 ± 1200 M^{-1} s^{-1}
r	0.996

[a] For an ionic strength of 0.1 M at 25 °C.

Any viable mechanism for the bromination of 2-AP must be in accordance with the observed kinetics, the pH dependence of the rate, and the formation of the observed intermediate. As mentioned in the Introduction, the reaction of 2-AP with bromine in water leads initially to the formation of an addition intermediate, **6**, rather than a substitution product (Scheme 6.2). This formation has been confirmed by new NMR experiments described in the Experimental section. Conceivably, the intermediate **6** could arise from bromine attack followed by water attack and addition, as in Scheme 6.3.

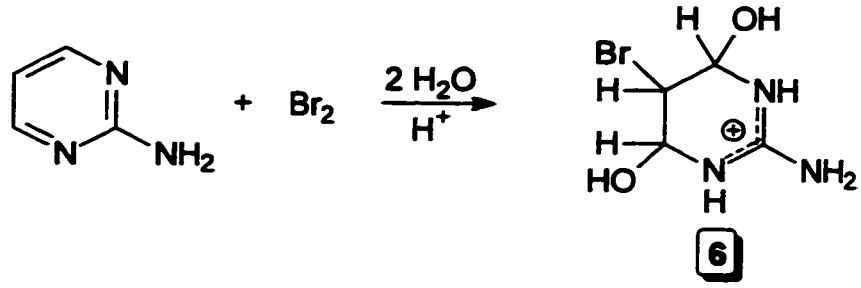

Scheme 6.2 Formation of the intermediate in the bromination of 2-AP.

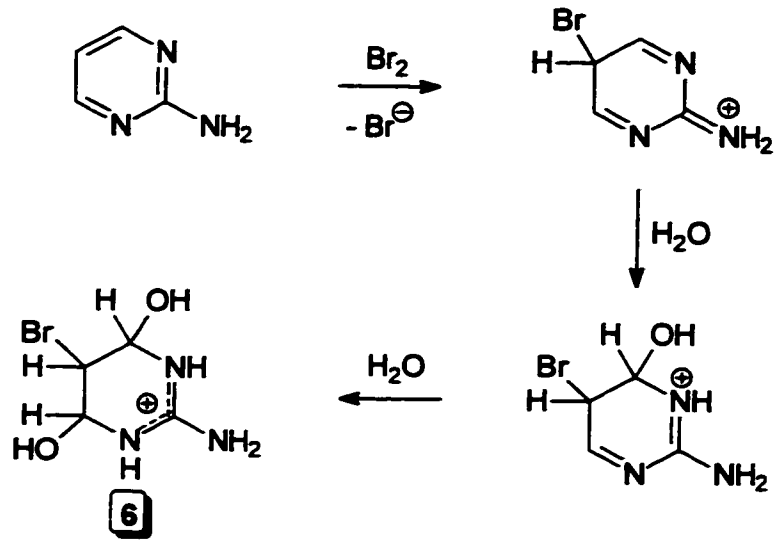

Scheme 6.3 Bromine attack followed by water attack and addition.

Alternatively, there could be the addition of water to 2-AP, followed by bromine attack and water attack (Scheme 6.4). A similar mechanism has been shown for the bromination of 2- and 4-pyrimidone.[55] Part of the object of this work was to try to differentiate between the two pathways in Scheme 6.3 and 6.4.

The mechanism in Scheme 6.4 could follow the pathway described below. Addition of water to the free base form **1**, probably via the cation **2**, can give **4** or **5**. Of the three hydrated species (**3**, **4**, and **5**), the cation **3** would be dominant at a low pH. However, structures **4** and **5** are strong guanidine-type bases and should be very reactive towards bromine. Structure **5** is in gray to illustrate that the paths leading from structures **4** and **5** are kinetically equivalent. In contrast, the path from the protonated form **3** would have a different dependence on the pH. Attack of bromine on **3**, **4** or **5**, followed by addition of a second water molecule, would yield the observed intermediate **6**.

The k'_2 value of 2.5×10^4 M^{-1} s^{-1} obtained for the bromination of 2-AP at pH 3 - 6 agrees with the range of values predicted for bromine attack on 2-AP in the previous section. Therefore, the reaction of 2-AP seems to occur, at least in part, in the same fashion as the bromination of aniline and 2-APy, by direct attack of bromine, as in Scheme 6.3.

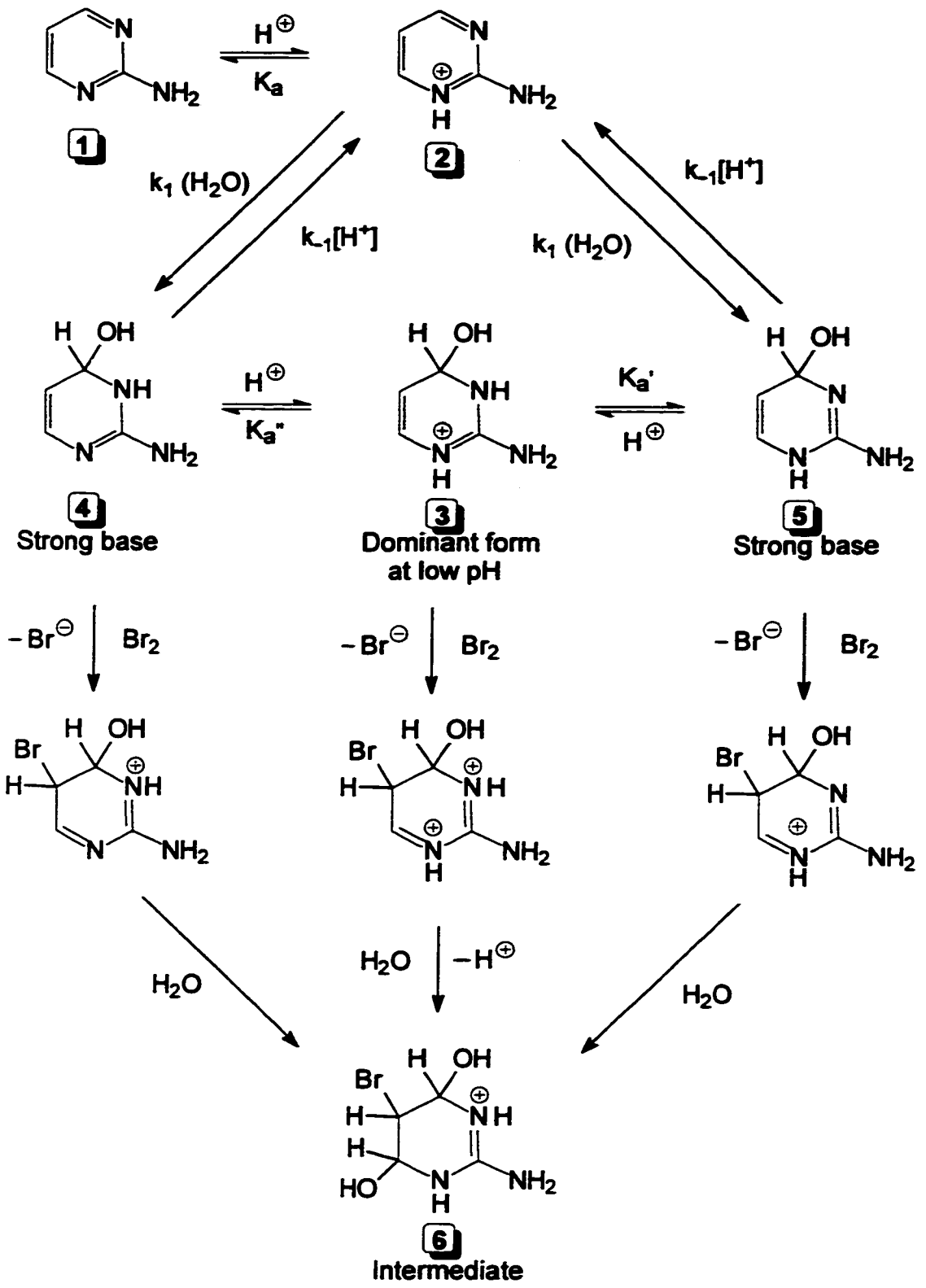

Scheme 6.4 Proposed mechanism for the bromination of 2-aminopyrimidine.

At lower pH values (pH < 2), another mechanism is taking place and it is harder to explain what is happening. The mechanism in Scheme 6.4 is complex because there are several equilibria involved. Of course, there is an equilibrium between the two forms of the substrate, **1** and **2**, but there may be small amounts of the hydrated cation **3** and its free base forms **4** and **5**. Since the pH rate profile for the bromination is flat at pH < 2 (Figure 6.6) the reactive species must be the protonated form **2** *or some other protonated form in equilibrium with it*, most probably the hydrated form **3** (Scheme 6.4). Support for the idea that the reactive form is the cation **3**, in equilibrium with the cation **2**, comes from observations made for the cation **7** (Scheme 6.5) which reacts with an observed second order rate constant of 1000 M^{-1} s^{-1}, very close to the value of 1200 M^{-1} s^{-1} for **2**. So, it is proposed that **2** reacts via the hydrated form **3**, and **7** reacts via its hydrated form **10** (Scheme 6.5).

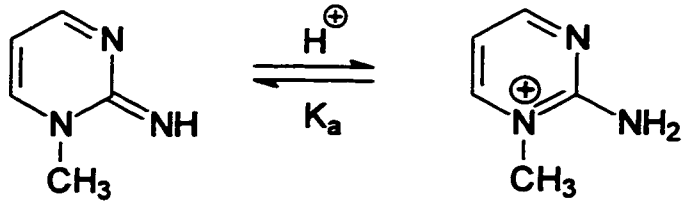

M2A **7**

Because it is a guanidine, 1,2-dihydro-2-imino-1-methyl pyrimidine (M2A) is very basic, with a pK_a of 10.75[56], and it exists as its cation **7** at all pHs studied. We chose to study this system because the cation **7** could serve as a model of the protonated form of 2-AP, **2**.

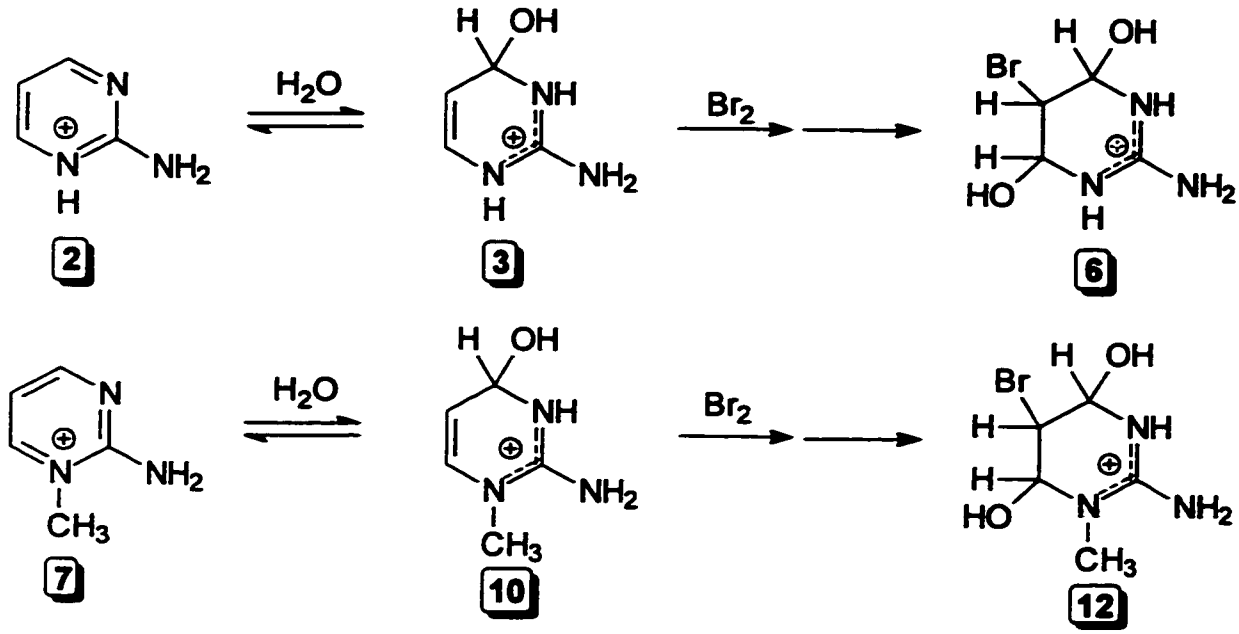

Scheme 6.5 Suggested pathways for the bromination of 2-AP and M2A.

The pH rate profile for the bromination of M2A is very interesting and quite complex, as seen in Figure 6.7. Assuming that this pyrimidine reacts with bromine in a similar way as 2-AP, at least two mechanisms must be involved, one at low pH (0 to 3.5) and one or more at higher pH (4 to 7). At low pH, the pH rate profile for **7** is almost identical to the pH rate profile for the bromination of 2-AP, therefore we propose a similar mechanism as for 2-AP, as shown in Scheme 6.5. Since M2A is very basic[56], the cation **7** of the substrate is the predominant form in solution, but structures **8** and **10** could be available due to pre-equilibrium hydration, which leaves the rate determining step to be the attack by bromine. Bromine attack on the cation **10** could explain the pH-rate profile (Figure 6.7) at low pH.

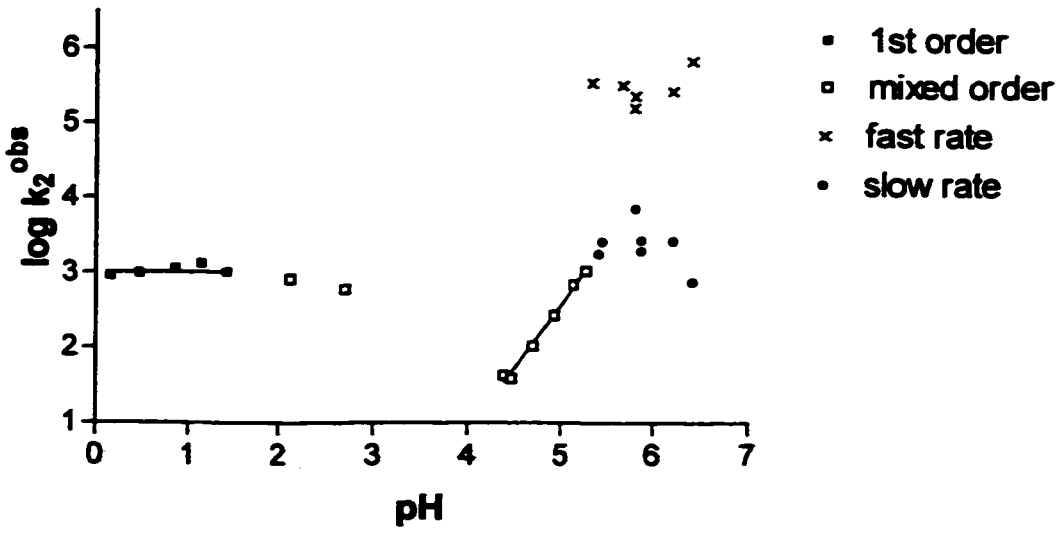

Figure 6.7 pH rate profile for the bromination of 1,2-dihydro-1-imino-1-methyl pyrimidine.

Around pH 2, we observe a transition from first-order kinetics (Figure 6.8 (a)) through mixed order (b) to zero-order (c). Again, similar behaviour was observed previously for the bromination of 2- and 4-pyrimidones.[55] The change in order is consistent with a change of rate-limiting step from bromine attack to hydrate formation. To understand where these different orders arise from, kinetic equations may be explored.

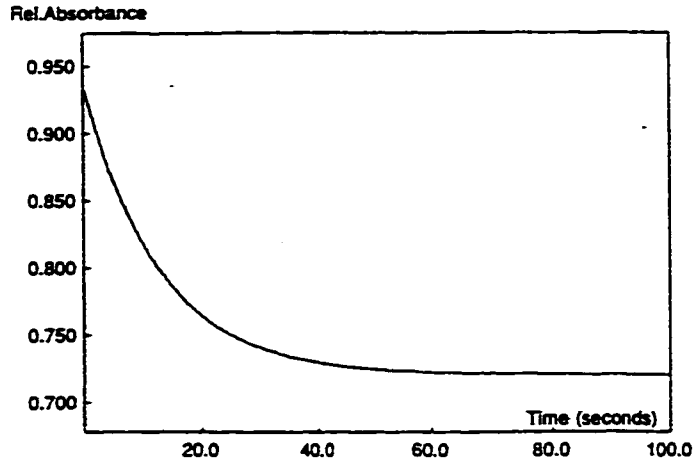

(a) pH = 0.465

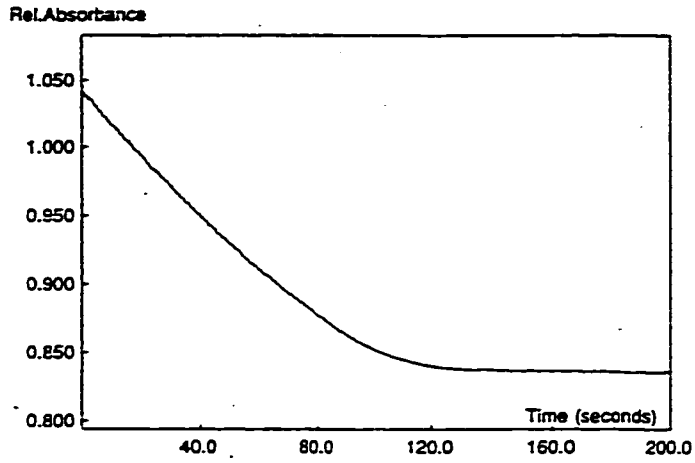

(b) pH = 2.12

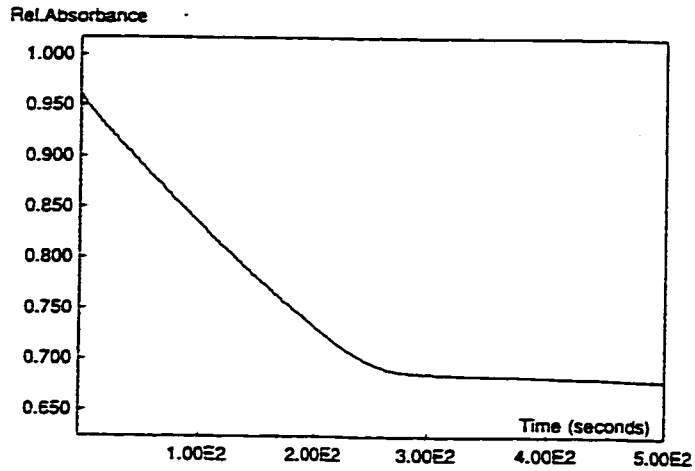

(c) pH = 2.95

Figure 6.8 Traces of (a) first-order kinetics, (b) mixed-order kinetics and (c) zero-order kinetics

We have considered the following possibility:

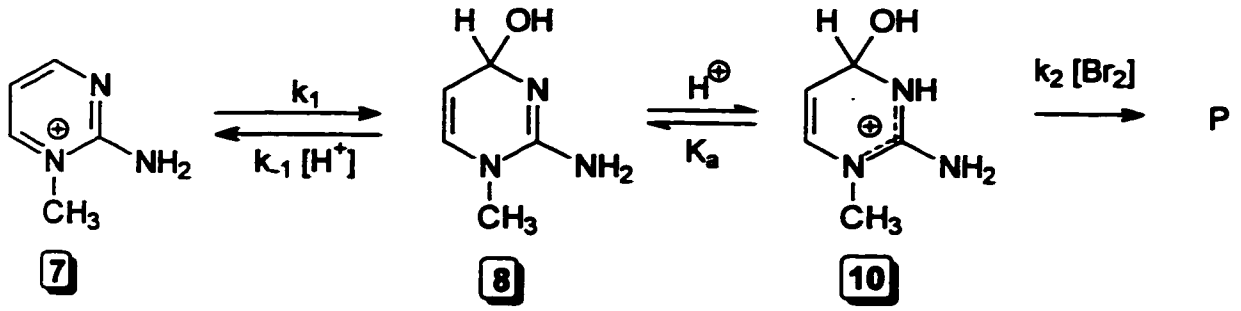

Scheme 6.6

The total amount of **8** will be found in two forms, namely, **8** and **10**, but since **8** is a very strong base, we can make the following assumption.

$$[8]_t = [8] + [10] \approx [10] \tag{3.6}$$

and

$$[8] = [10]\, K_a / [H^+] \tag{3.7}$$

We followed the reaction by monitoring the disappearance of bromine and according to Scheme 6.6 the rate is given by:

$$\text{rate} = \frac{-d[Br_2]}{dt} = k_2\,[10]\,[Br_2] \tag{3.8}$$

As long as **8** and **10** are in rapid equilibrium,

$$\frac{d\,[10]}{dt} \approx \frac{d\,[8]}{dt} \tag{3.9}$$

$$= k_1\,[7] - k_{-1}\,[8]\,[H^+] - k_2\,[10]\,[Br_2] \tag{4.0}$$

and substituting for [8] from (3.7)

$$= k_1[7] - k_{-1}\frac{[10]K_a}{[H^+]}[H^+] - k_2[10][Br_2] \qquad (4.1)$$

Using the steady state assumption on (**8** ⇌ **10**) equation 4.1 = 0, and so we can isolate [**10**].

$$[10] = \frac{k_1[7]}{k_{-1}K_a + k_2[Br_2]} \qquad (4.2)$$

Substituting for [**10**] in equation 3.8 yields

$$\text{rate} = \frac{k_1 k_2[7][Br_2]}{(k_{-1}K_a + k_2[Br_2])} \qquad (4.3)$$

The above rate equation *cannot* explain a change of rate-limiting step near pH 2 with pH because it has no term in [H^+] (or [OH^-]) in the denominator. Accordingly, the mechanism in Scheme 6.6 is not viable.

Consider now, another possibility.

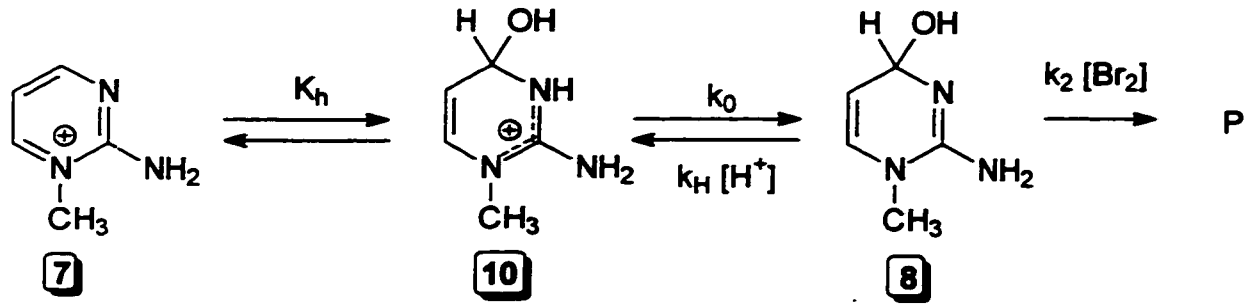

Scheme 6.7

In this mechanism the cation **10** is formed in a pre-equilibrium from **7**, and the free base form **8** is formed from **10**. However, **8** is a strong, guanidine-type base which would form slowly from **10** *and* it is an enamine so it should react rapidly with

bromine. We will consider **8** as a steady-state intermediate:

$$\frac{d[8]}{dt} = k_0[10] - k_H[8][H^+] - k_2[8][Br_2] = 0 \qquad (4.4)$$

and so,

$$[8] = \frac{k_0[10]}{k_H[H^+] + k_2[Br_2]} \qquad (4.5)$$

But $K_h = [10] / [7]$, and $[10] = K_h[7]$

Thus, according to Scheme 6.7 the rate of bromination is

$$-d[Br_2]/dt = k_2[8][Br_2] \qquad (4.6)$$

$$= \frac{k_0 K_h k_2 [7][Br_2]}{(k_H[H^+] + k_2[Br_2])} \qquad (4.7)$$

For the rate equation in (4.7) there are two extreme situations.

(i) $k_H[H^+] >> k_2[Br_2]$, in which case

$$\frac{-d[Br_2]}{dt} = \frac{k_0 K_h k_2 [7][Br_2]}{k_H[H^+]} \qquad (4.8)$$

This situation corresponds to rate-limiting attack of bromine on **8**, and it requires first order kinetics for high [**7**] and fixed $[H^+]$. The corresponding pseudo-first order rate constant ($= k_0 K_h k_2 [7] / k_H[H^+]$) should increase with increasing pH.

(ii) $k_2[Br_2] >> k_H[H^+]$. In this case, the acidity is low enough that reprotonation of **8** to **10** cannot compete with fast bromine attack and

$$-d[Br_2]/dt = k_0 K_h [7] \qquad (4.9)$$

In other words, the formation of **8** is the rate-limiting step and the kinetics are pseudo-zero order.

Overall, Scheme 6.7 and its rate equation (4.7) require the pseudo-first order rate constant to vary with $1/[H^+]$ at high $[H^+]$ whereas at low $[H^+]$ there should be pseudo-zero-order behaviour and no pH dependence. Unfortunately, such behaviour was not observed.

The third and final possibility that will be considered is the mechanism shown in Scheme 6.8.

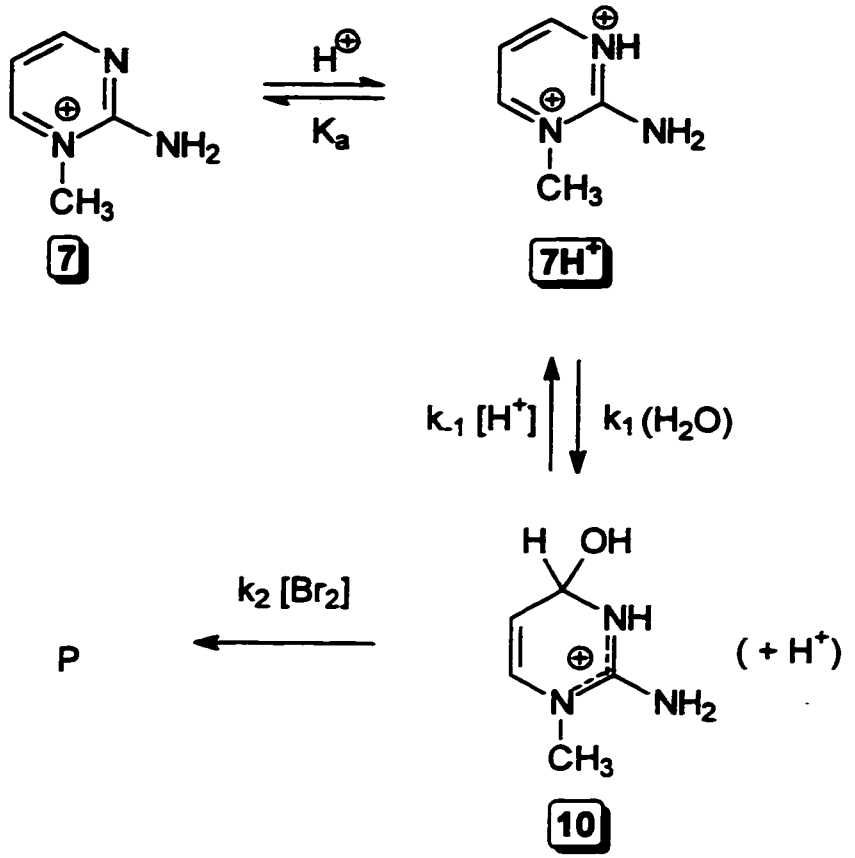

Scheme 6.8

For this scheme,

$$\text{rate} = k_2\,[\mathbf{10}]\,[Br_2] \qquad (5.0)$$

Using the steady state assumption on **10**:

$$d\,[\mathbf{10}] / dt = k_1\,[\mathbf{7H^+}] - k_{-1}\,[\mathbf{10}]\,[H^+] - k_2\,[Br_2]\,[\mathbf{10}] = 0 \qquad (5.1)$$

$$[\mathbf{10}] = \frac{k_1\,[\mathbf{7H^+}]}{k_{-1}\,[H^+] + k_2\,[Br_2]} \qquad (5.2)$$

However, $$[\mathbf{7H^+}] = [\mathbf{7}]\,[H^+] / K_a \qquad (5.3)$$

and, substituting for [**10**] and [**7H$^+$**]

$$\text{rate} = \frac{k_1\,[\mathbf{7}]\,[H^+]\,k_2\,[Br_2]}{K_a\,(k_{-1}\,[H^+] + k_2\,[Br_2])} \qquad (5.4)$$

This rate equation, which is appropriate for the mechanism in Scheme 6.8, *can* explain the pH-rate profile for the bromination of **7** in the pH range 0 - 3.

At low pH, if $k_{-1}\,[H^+] >> k_2\,[Br_2]$ then this equation (5.4) simplifies to

$$\text{rate} = \frac{k_1\,[\mathbf{7}]\,[H^+]\,k_2\,[Br_2]}{K_a\,k_{-1}\,[H^+]} \qquad (5.5)$$

$$= \frac{k_1\,[\mathbf{7}]\,k_2\,[Br_2]}{K_a\,k_{-1}} \qquad (5.6)$$

Equation (5.6) has no dependence on the [H$^+$], and it corresponds to rate-limiting attack of bromine on the hydrated cation **10**, formed in a pre-equilibrium from the cation **7**. This mechanism is exactly that proposed earlier in Scheme 6.5.

At higher pH, if $k_2\,[Br_2] >> k_{-1}\,[H^+]$ then

$$\text{rate} = \frac{k_1\,[\mathbf{7}]\,[H^+]}{K_a} \qquad (5.7)$$

Equation (5.7) has a [H$^+$] term in the numerator and therefore the rate would decrease with increasing pH. Since this equation is zero-order with respect to bromine, the rate-limiting step involves the formation of **10** by water attack on **7H$^+$**.

Thus, the mechanism presented in Scheme 6.8 and the rate equation (5.4) can explain the observed change in rate-limiting step. At first glance, the dication

$7H^+$ is not easy to conceive, but it is not far-fetched since double protonation has been observed in the case of 6-amino-2,4-dimethylpyrimidine (6-ADP) (pK_1 = 6.90; pK_2 = -0.14).[57]

By observing the pH rate profile for the bromination of 2-AP (Figure 6.6), one can see that two points (□) were not taken into account to estimate the pK_a value. These points were not taken into account because mixed order kinetics were observed at a pH of about 2.3 - 2.5. If we consider applying a similar mechanism as in Scheme 6.8 to 2-AP, we must consider the possibility of a dication. A dication could be viable if we think in terms of pK_1 and pK_2. By comparison with 6-ADP, 2-AP should have a pK_1 ≈ 3.50 and pK_2 ≈ -2 or -3, which is not far from the pHs at which we performed the experiments. It seems likely that there is also a change of rate-limiting step in the bromination of the cation of 2-AP, near pH 2.5, but the zero order process never becomes truly established because attack of bromine on the free base form of 2-AP takes over at pH > 2.5 (Figure 6.6).

Returning to the subject of the bromination of **7**, at higher pH (4 - 7), the pH rate profile is complex, in addition to the various orders obtained two unexpected results were noticed. First, in the pH region of 4.5 to 6 for log k_2^{obs} vs pH a slope of ~ 1.7 was calculated, which suggests that two protons are removed in the reaction. In the case of the bromination of 2-AP a slope of ~ 1 had been calculated. The second surprise was that two different rates could be observed at the highest pHs. A very rapid rate and a slow rate were seen. For the moment, we cannot explain these various observations, and further experiments, with the same compound and

with similar derivatives, will have to be carried out to resolve this enigma.

The only problem with performing other experiments is the reproducibility factor. While working with the various substrates (aniline, *N,N*-dimethylaniline, 2-APy, 2-DAPy, 2-ADP and 2-AP), the results obtained were easily reproduced, whereas in the case of M2A reproducibility was very hard to attain. In a science where precision is a key factor, substrates like M2A can make our work tedious and interesting at the same time.

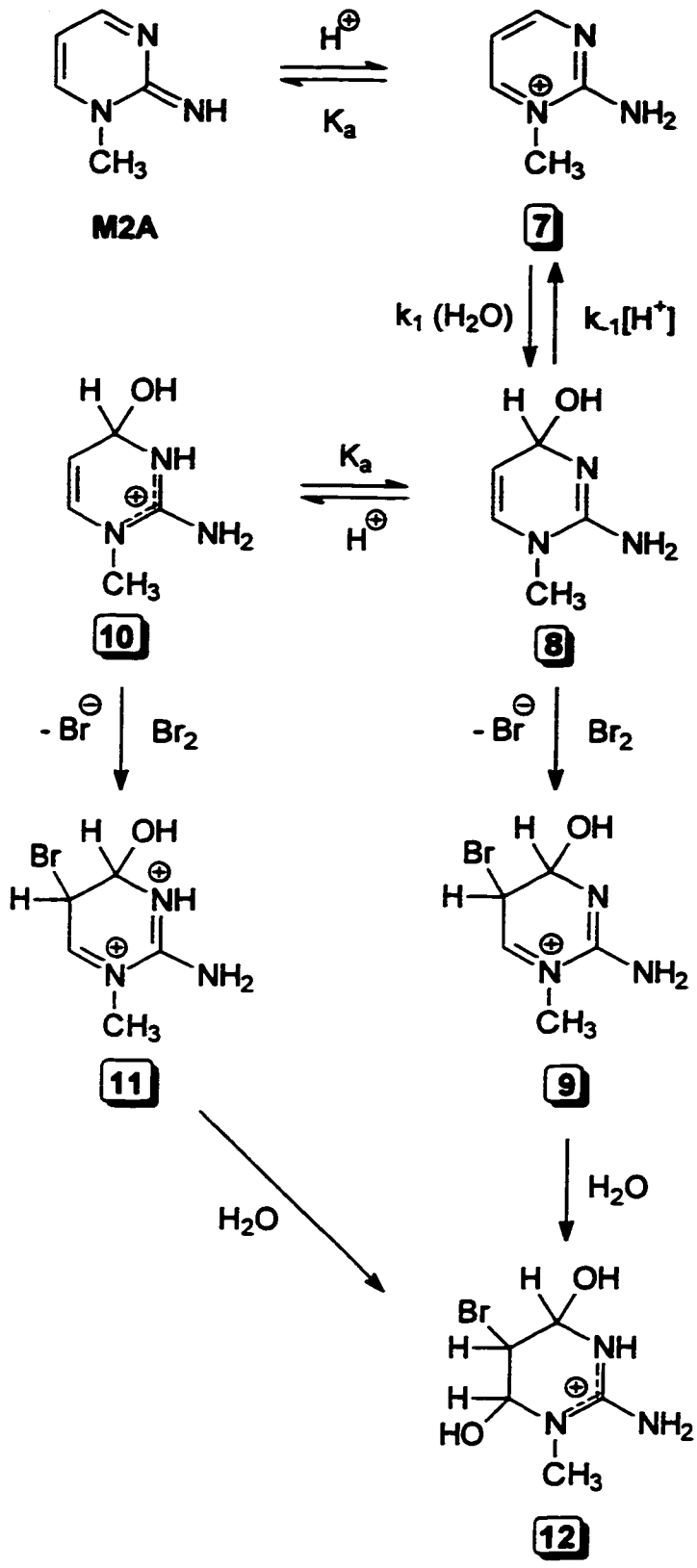

Scheme 6.9 Proposed mechanism for the bromination of M2A.

7. Conclusion

Direct bromination seems to be involved for the bromination of aniline, *N,N*-dimethylaniline, 2-DAPy, 2-APy and 2-ADP. These substrates exhibit a simple linear relationship between log k_2^{obs} and pH. The pH rate profile of the bromination of 2-AP is slightly more complex as it is a sigmoidal curve. A mechanism for the bromination of 2-AP was proposed that agrees with the data collected. A similar mechanism was proposed for the bromination of M2A. Further experiments will have to be performed to determine whether the mechanism is proper. The pH rate profile of the bromination of M2A was unusual, leading to mixed observations. New substrates should be studied to further investigate the mechanism involved. As an example, 2-amino-4-methylpyrimidine is available in the laboratory. It would also be interesting to perform substituent effect studies to evaluate the effect of the presence or absence of a single nitrogen group or both nitrogen groups in the aromatic ring.

8. Experimental

8.1 Materials

2-Aminopyrimidine, 2-amino-4,6-dimethylpyrimidine, 2-aminopyridine, 2-dimethyl aminopyridine, aniline, *N,N*-dimethylaniline and the bromine were purchased from Aldrich Chemical Co. 2-Aminopyrimidine and 2-amino-4,6-dimethylpyrimidine were recrystallized previous to their use. Standard HCl solutions were obtained from A & C Chemicals (Montréal).

1:2-Dihydro-2-imino-1-methylpyrimidine (M2A) hydriodide was synthesized by methylation of 2-aminopyrimidine following Brown et al..[39] A total yield of 64.7 % was obtained. The corresponding perchlorate salt was synthesized following Tee et al. procedure.[40] The total yield obtained was 79.3%. The ^{1}H NMR shifts are shown in Table 8.2. The ^{1}H NMR chemical shifts are almost identical for the reference compound (M2A) as for the newly synthesized M2A.

8.2 Kinetic Experiments

The kinetic experiments were carried out by using a single beam stopped-flow spectrophotometer by Applied Photophysics model SX17MV. Bromination was followed by monitoring absorbance decrease at 267 nm (tribromide ion band) for the disappearance of bromine. In the stopped-flow apparatus the mixing is 1:1 and so the concentrations before and after mixing differ by a factor of 2. The observation cell was kept at 25.0 ± 0.1 °C. Bromine solutions were prepared in 0.1 M KBr to maintain the ionic strength.

Table 8.1 Parameters for Bromination

Compound	$[Br_2]_0$ used,M	[substrate] used before mixing, M
2-AP	5×10^{-5}	2×10^{-3}
	1×10^{-4}	
2-ADP	5×10^{-5}	2×10^{-3}
M2A	5×10^{-5}	5×10^{-4}
	1×10^{-4}	
2-APy	1×10^{-4}	2×10^{-3}
2-DAPy	5×10^{-5}	2×10^{-3}
aniline	5×10^{-5}	2×10^{-3}
N,N-dimethylaniline	5×10^{-5}	1×10^{-3}

For the pH range of 0.15 to 2.12, HCl solutions were used. For the pH range of 2.20 to 3.40 chloroacetic buffers were used. For pH between 4.10 to 5.30, acetate buffers were used. And finally for pH between 6.40 to 7.70 phosphate buffers were used. Succinic buffers were used for a pH range of 4.40 to 5.90.[a]

[a] Succinic buffer reacts slowly with bromine, and to prevent any problems the buffer was only added to the substrate.

8.3 Calculations of Rate Constants

With the instrument manufacturer's software, the observed first order rate constants (k_{obs}) were calculated by fitting the absorbance trace with a single exponential. The absorbance traces were composed of 400 points. The trace analyzed was an average of 5 - 10 individual traces. In some cases the trace exhibited different or mixed orders, when this occurred the absorbance trace was fitted with two exponentials or a linear portion followed by a single exponential.

From the observed rate constants, the second order rate constants were calculated using a spreadsheet (see Appendix B). A value of k_2^{app} is calculated by dividing k_1^{obs} by ([substrate] - $[Br_2]_b$) for reasons given earlier.[58] Then k_2^{obs} is obtained by dividing k_2^{app} by the fraction of Br_2 present in solution. The free bromine in solution is influenced by two equilibria: i) formation of tribromide ion (eq. 8.1); ii) hydrolysis to hypobromous acid (eq. 8.2).

$$Br_2 + Br^- \underset{}{\overset{K_1}{\rightleftharpoons}} Br_3^- \qquad (8.1)$$

$$Br_2 + H_2O \underset{}{\overset{K_2}{\rightleftharpoons}} H^+ + Br^- + HOBr \qquad (8.2)$$

For these equilibria, the constants[59,60] are:

$$K_1 = \frac{[Br_2][Br^-]}{[Br_3^-]} = 5.62 \times 10^{-2}\ M \qquad (8.3)$$

$$K_2 = \frac{[H^+][Br^-][HOBr]}{[Br_2]} = 9.60 \times 10^{-9}\ M^2 \qquad (8.4)$$

In fact, under the reaction conditions used, the correction for HOBr is only significant at pH > 5.

The fraction of Br_2 is calculated using these dissociation constants, the [Br^-] and [H^+] and equation (8.3).

$$\frac{[Br_2]_t}{[Br_2]} = 1 + \frac{[Br^-]}{K_1} + \frac{K_2}{[H^+][Br^-]} \qquad (8.5)$$

In each case where the first-order disappearance of bromine was observed,

$$\text{rate} = \frac{-d[Br_2]}{dt} = k_1^{obs}[Br_2] \qquad (8.6)$$

and it was verified that the reactions were also first order in substrate:

$$\text{rate} = k_1^{obs}[Br_2] = k_2^{obs}[S][Br_2] \qquad (8.7)$$

In other words, k_1^{obs} values vary with [substrate]. The relevant data are given in the Appendix B.

8.4 pK_a Estimation

The pK_a of 2-DAPy was estimated by titrating a 0.05 M solution of 2-DAPy with a 0.10 M HCl solution at 22 °C. The experiment was carried out by monitoring the pH change using an Accumet model 25 pH/ion metre by Fisher Scientific. The calculations were carried using a Lotus 1-2-3 spreadsheet, based on the method described by Albert and Serjeant.[45]

8.5 Observation of the Bromination of 2-AP intermediate by ^1H NMR

Approximately 0.005 moles of 2-AP (~ 0.47 g) was dissolved in 5 ml solution of 2 M DCl in D_2O. The DCl solution was prepared by adding ~ 1 g of 37 wt% DCl (F.W. 37.47) in D_2O and diluting to the 5 ml mark with D_2O. The bromine solution

was prepared by adding 0.005 moles (~ 0.79 g) of bromine to 5 ml of D_2O. Approximately 0.5 ml of the 2-AP solution was mixed in a NMR tube with 0.5 ml of the bromine solution and a ^1H NMR spectrum was ran. In addition to the two 2-AP peaks found at 8.65 and 7.15 ppm, two peaks characteristic of the intermediate appeared upfield at 5.33 and 4.49 ppm (Table 8.2). By adding more bromine and therefore saturating the mixture, the ^1H NMR spectrum showed that the intermediate peaks increased and the starting material peaks disappeared.

Table 8.2. ^1H NMR Shifts

Compound	Solvent	Chemical Shifts, ppm 4H	5H	6H	N-CH_3	J, Hz
M2A (ref.)	D_2O	8.36 (dd)	7.09 (dd)	8.79 (dd)	3.84 (s)	J_4 = 2.1, 4.5; J_5 = 2.1, 4.35; J_6 = 1.95, 3.6
M2A (new)	D_2O	8.36 (dd)	7.08 (dd)	8.79 (dd)	3.84 (s)	J_4 = 2.1, 4.8; J_5 = 2.1, 4.6; J_6 = 2.1, 2.4
2-AP	2M DCl/D_2O	8.65 (d)	7.15 (t)	8.65 [a] (d)	-	$J_{4,6}$ = 5.4; J_5 = 5.4, 6.3
2-AP (inter.)[b]	1M DCl/D_2O	5.32 (d)	5.14 (t)	5.32 [a] (d)	-	$J_{4,6}$ = 2.1; J_5 = 1.2, 2.7

[a] Same as 4H.
[b] The intermediate in the bromination of 2-AP, as explained in the Experimental Section.

References

1. D. J. Cram, *Angew. Chem. Int. Ed. Engl.*, **27**, 1009, **1988**.
2. J.-M. Lehn, *Science*, **227**, 849, **1985**.
3. J. Szejtli, *Cyclodextrins and their Inclusion Complexes*, Akadémiai Kiadó, Budapest, **1982**.
4. M. L. Bender and M. Komiyama, *Cyclodextrin Chemistry*, Springer-Verlag, New York, **1978**.
5. *Proceedings of the First International Symposium on Cyclodextrins*, J. Szejtli (Ed.), D. Reidel Publishing Company, Boston, **1982**.
6 B. Alberts, D. Bray, J. Lewis, M. Raff, K. Roberts, J. D. Watson, *Molecular Biology of the Cell, 3rd ed.*, Garland Publishing, New York, **1994**, pp. 89-97
7. H.-J. Schneider, *Angew. Chem. Int. Ed. Engl.*, **30**, 1417, **1991**.
8. A. Lehninger, D. Nelson, M. Cox, *Principles of Biochemistry, 2nd ed.*, Worth Publisher, New York, **1993**, p. G-4
9. O. S. Tee, *Adv. Phys. Org. Chem.*, **29**, 1, **1994**.
10. O. S. Tee, R. A. Donga, *J. Chem. Soc., Perkin Trans. 2*, 2763, **1996**.
11. E. Cordes, H. Bull, *Chem. Rev.*, **74**, 581, **1974**.
12. O. S. Tee, A. A. Fedortchenko, P. Lim Soo, *J. Chem. Soc., Perkin Trans. 2*, 123, **1998**.
13. I. E. Turner, *The Effect of Cyclodextrins on the Hydrolysis of Trimethyl Orthobenzoate and its use to Probe Guest Binding*, CHEM 450 Research

project & Thesis, Concordia University, **1997**.

14. a) O. S Tee, T. A. Gadosy and J. B. Giorgi, *Can. J. Chem.*, **74**, 736, **1996**. b) O. S Tee, A. A Fedortchenko, P. G. Loncke, T. A. Gadosy, *J. Chem. Soc., Perkin Trans. 2*, 1243, **1996**.
15. Y. Matsui, T. Nishioka and T. Fujita, *Top. Curr. Chem.*, **128**, 61, **1985**.
16. W. Hirsch, T. Muller, R. Pizer, P.J. Ricatto, *Can. J. Chem.*, **73**, 12 , **1995**.
17. F. Hacket, J.-M. Coteron, H.-J. Schneider, V.P. Kazachenko, *Can. J. Chem.*, **75**, 52, **1997**.
18. Y. Aoyama, Y. Nagai, J.-I. Otsuki, K. Kobayashi, H. Toi, *Angew. Chem. Int. Ed. Engl.*, **31**, 745, **1992**.
19. A.F. Danil de Namor, P.M. Blackett, M.C. Cabaleiro, J.M. Al Rawl, *J. Chem. Soc. Farady Trans.*, **90**, 845, **1994**.
20. J. McMurry, *Organic Chemistry, Third Edition*, Brooks/Cole, Pacific Grove, **1992**.
21. D. J. Brown, *The Pyrimidines*, Vol. 16 of *The Chemistry of Heterocyclic Compounds*, A. Weissberger Ed., Interscience, New York, **1962**.
22. D. J. Brown, E. Hoerger, S. F. Mason, *J. Chem. Soc.*, 4035, **1955**.
23. A. R. Katritzky, M. Kingsland and O. S. Tee, *J. Chem. Soc. (B)*, 1484, **1968**.
24. S. Banerjee, *The Mechanism of Bromination of Mono- and Dioxo-Pyrimidines*, M.Sc. Thesis, Sir George Williams University, **1974**.
25. F. Platis, *Bromination of 2-Aminopyrimidine and Related Compounds*, CHEM 450, Concordia University, **1980**.

26. W. Barbieri, L. Bernardi, G. Palamidessi, and M. T. Venturi, *Tetrahedron Lett.*, 2931, **1968**.

27. R. A. Barnes, F. Brody, and P. R. Ruby, *Pyridine and Its Derivatives, Part One*, Vol. 14 of *The Chemistry of Heterocyclic Compounds*, A. Weissberger Ed., Interscience, New York, **1960**.

28. H. E. Mertel, R. H. Mizzoni, E. N. Shaw, L. E. Tenenbaum, and H. L. Yale, *Pyridine and Its Derivatives, Part Two*, Vol. 14 of *The Chemistry of Heterocyclic Compounds*, A. Weissberger Ed., Interscience, New York, **1961**.

29. J. P. Wibaut, G. M. Kraay, *Rec. Trav. Chim.*, 1085, **1924**.

30. A. E. Tschitschibabin, I. L. Knunianz, *Ber.*, **61**, 427, **1928**.

31. R. S. Shallenger and G. G. Birch, *Sugar Chemistry*, Avi Publishing Company, Wesport, **1975**.

32. R. J. Ferrier and P. M. Collins, *Penguin Library of Physical Sciences, Monosaccharide Chemistry*, Penguin Education, Middlesex, **1972**.

33. H. S. El Khadem, *Carbohydrate Chemistry, The Monosaccharides anf Their Oligomers*, Academic Press, San Diego, **1988**.

34. R. D. Guthrie and J. Honeyman, *Introduction to Carbohydrate Chemistry, Fourth Edition*, Clarendon Press, Oxford, **1974**.

35. R. S. Shallenberger, *Advanced Sugar Chemistry, Principle of Sugar Stereochemistry*, Avi Publishing Company, Westport, **1982**.

36. R. P. Bell and E. N. Ramsden, *J. Chem. Soc.*, 161, **1958**.

37. P. J. Brignell, P. E. Jones and A. R. Katritzky, *J. Chem. Soc. (B)*, 117, **1970**.

38. *Handbook of Biochemistry and Molecular Biology, Third ed., Physical and Chemical Data, Volume I*, G. D.Fasman (Ed.), CRC Press, Cleveland, **1976**.

39. D.J. Brown, E. Hoerger and S.F. Mason, *J. Chem. Soc.*, 4035, **1955**.

40. O.S. Tee and S. Banerjee, *J. Org. Chem.*, **44**, 18, 3256, **1979**.

41. D.W. Griffiths and M.L. bender, *Adv. Catalysis*, **23**, 209 **1973**.

42. J.H. Fendler and E.J. Fendler, *Catalysis in Micellar and Macromolecular Systems*, Academic Press, New york, **1975**.

43. M. Komiyama and M.L. Bender, *The Chemistry of Enzyme Action*, M.I.Page, Ed., Elsevier, Amsterdam, **1984**.

44. O.S. Tee, *Carbohydr. Res.*, **192**, 181 **1989**.

45. A. Albert and E.P. Serjeant, *The Determination of Ionization Constants, A Laboratory Manual*, 3rd Edition, Chapman and Hall, New York, **1984**.

46. S. Hussain, *Inhibition and Catalysis Effects of Cyclodextrins*, CO-OP Work Term Report, Concordia University, **1997**.

47. X. Du, *The Cleavage of Aryl Alkanoates Esters by Cyclodextrins*, M. Sc. Thesis, Concordia University, **1989**.

48. A.A. Fedortchenko, *Stabilization of Transition States of Organic Reactions by Cyclodextrins, Micelles, and Dendrimers*, M.Sc. Thesis, Concordia University, **1997**.

49. A. A. Fedortchenko, Ph. D., work in progress.

50. Patrick Lim Soo, *The Retardation of Acetal Hydrolysis by Cyclodextrins and*

its use in Probing Cyclodextrin-guest binding, CHEM 450 Research project & Thesis, Concordia University, **1997**.

51. K.A. Connors, *Binding Constants, The Measurement of Molecular Complex Stability*, Wiley-Interscience Publication, New York, **1987**.

52. (*a*) I. Tabushi, K. Shimokawa, N. Shimizu, H. Shirakata and K. Fujita, *J. Am. Chem. Soc.*, **98**, 7855, **1976**; (*b*) I. Tabushi, N. Shimizu, T. Sugimoto, M. Shiozuka and K. Yamamura, *J. Am. Chem. Soc.*, **99**, 7100, **1977**; © Y. Matsui, K. Ogawa, S. Mikami, M. Yoshimoto and K. Mochida, *Bull. Chem. Soc. Jpn.*, **60**, 1219, **1987**; (*d*) Y. Aoyama, Y. Nagai, J. Otsuki, K. Kobayashi and H. Toi, *Angew. Chem., Int. Ed. Engl.*, **31**, 745, **1992**; (*e*) Y. Aoyama, J. Otsuki, Y. Nagai, K. Kobayashi and H. Toi, *Tetrahedron Lett.*, **33**, 3775, **1992**.

53. (*a*) O. S. Tee, *The Hydrogen-Deuterium Exchange of Some Simple Pyrimidines*, Ph.D. Thesis, University of East Anglia, **1967**; (*b*) A.R. Katritzky, M. Kingsland and O. S. Tee, *J. Chem. Soc. (B)*, 1484, **1968**.

54. (*a*) T. H. Lowry and K. S. Richardson, *Mechanism and Theory in Organic Chemistry, 2nd Edition*, Harper & Row, New York, **1981**, p. 131, Table 2.2; (*b*) Ibid, p. 132.

55. (*a*) O.S. Tee and S. Banerjee, *Can. J. Chem.*, **52**, 451, **1974**; (*b*) O.S. Tee and S. Banerjee, *J. Org. Chem.*, **44**, 18, 3256, **1979**; (*c*) O.S Tee and M. Paventi, *J. Org. Chem.*, **45**, 2072, **1980**; (*d*) O.S. Tee and M. Paventi, *J. Org. Chem.*, **45**, 2072, **1981**.

56. D.D. Perrin and I.H. Pitman, *J. Chem. Soc.*, 7071, **1965**.

57. K.L. Wierzchowski and D. Shugar, *Photochem. And Photobiol.*, **2**, 377, **1963**.

58. O.S. Tee and C.G. Berks, *J. Org. Chem.*, **45**, 830, **1980**.

59. R.P. Bell and E.N. Ramsden, *J. Chem. Soc.*, 1294, **1958**.

60. J.M. Pink, *Can. J. chem.*, **48**, 1169, **1970**.

APPENDIX A

Pentoses:

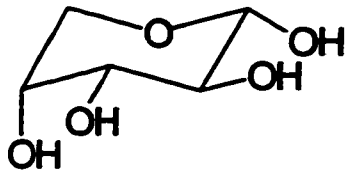

β-D-Arabinose
Pyranose form 97 %, Preferred conformation $^1C_4$

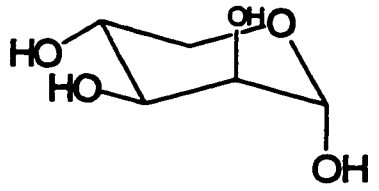

α-D-Lyxose
Pyranose form 99.5 %, Preferred conformation $^4C_1$

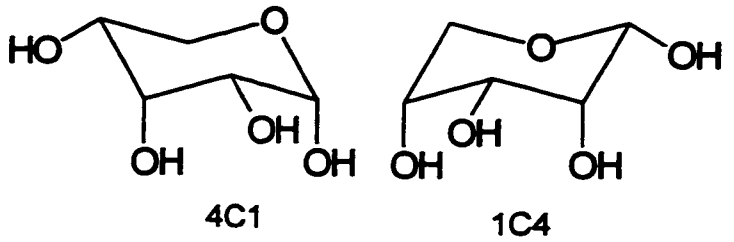

α-D-ribose
Pyranose form 76-80 %, No preferred conformation

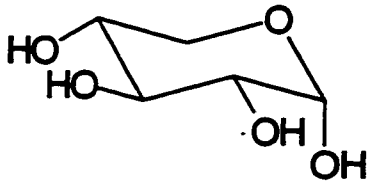

α-D-Xylose
Pyranose form 99.5 %, Preferred conformation $^4C_1$

Hexoses:

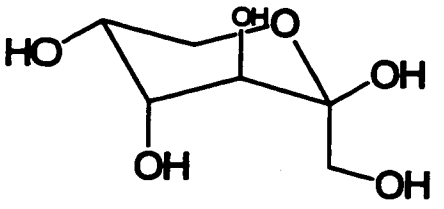

α-D-Fructose
Pyranose form 68.4 - 76.0 %, Preferred conformation $^4C_1$

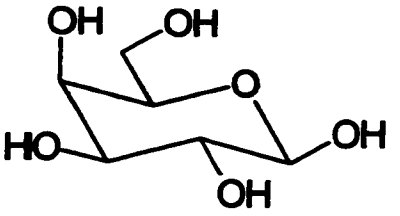

β-D-Galactose
Pyranose form 93 - 100%, Preferred conformation $^4C_1$

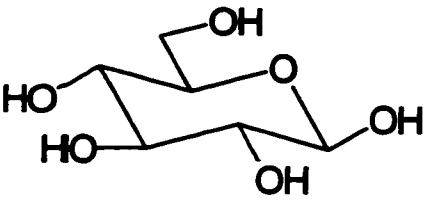

β-D-Glucose
Pyranose form 100%, Preferred conformation $^4C_1$

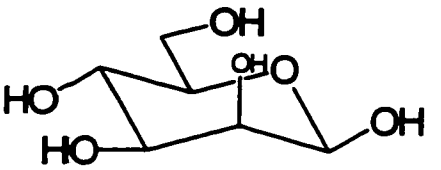

β-D-Mannose
Pyranose form 100%, Preferred conformation $^4C_1$

Others:

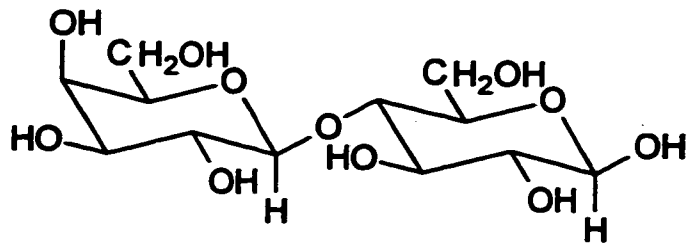

β-D-Lactose

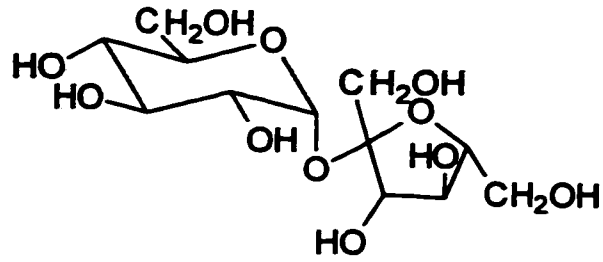

Sucrose

Alcohols:

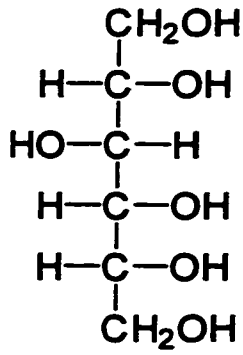

D-Sorbitol

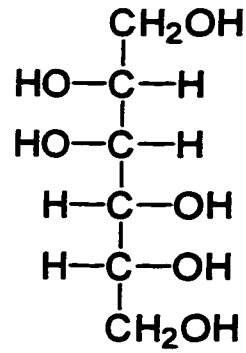

D-Mannitol

Sugars with uncertain configuration and/or conformation and/or anomer:

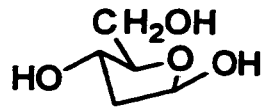

2-deoxy-D-ribose

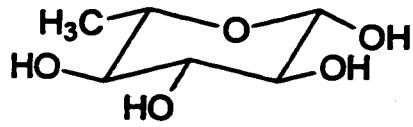

L-Rhamnose monohydrate

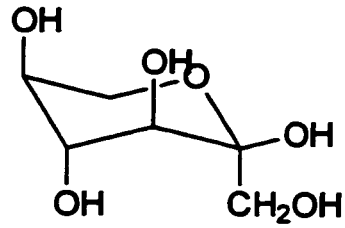

β-L-Sorbose

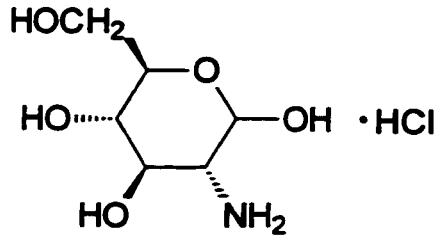

D-Glucosamine hydrochloride

APPENDIX B

Table B1.1. Raw Data for the Bromination ($[Br_2]_0$ = 0.0250 mM) of Aniline (1.00 mM) at 25°C.

Exp. #	pH	k_1^{obs}, s^{-1}	k_2^{obs}, s^{-1} M^{-1}
IT-190M	0.465	11.3	3.22×10^4
IT-195M	0.561	17.2	4.90×10^4
IT-194M	0.683	25.0	7.12×10^4
IT-189M	0.852	35.1	1.00×10^5
IT-193M	1.14	80.1	2.28×10^5
IT-192M	1.44	156	4.44×10^5
IT-191M	1.84	308	8.79×10^5
IT-198M	2.16	815	2.32×10^6

Table B1.1.1 Raw Data for the Dependence of k_1^{obs} on [Aniline] using $[Br_2]_0$ = 0.0250 mM at 25°C.

Exp. #	[Aniline] - $[Br_2]_0$, mM	k_1^{obs}, s^{-1}
IT-196M[a]	0.225	17.9
	0.475	35.3
	0.975	68.9
IT-197M[b]	0.225	8.37
	0.475	16.4
	0.975	32.9

[a] The experiments were performed at a pH of 1.14.
[b] The experiments were performed at a pH of 0.852.

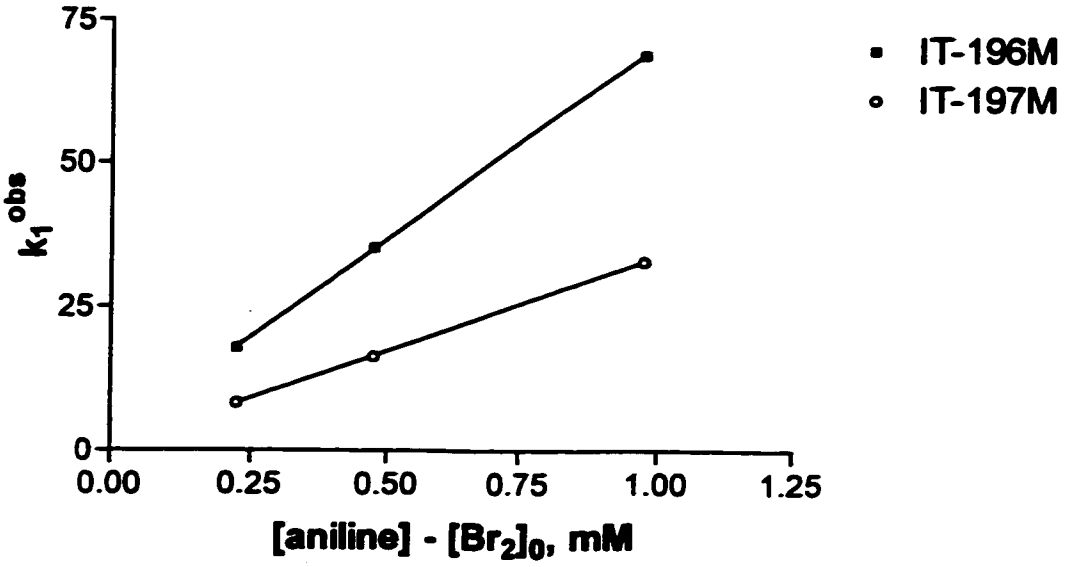

Figure B1.1.1 The Dependence of k_1^{obs} on the aniline concentration at a pH of 1.14 for experiment IT-196M and a pH of 0.852 for experiment IT-197M.

Table B1.2. Raw Data for the Bromination ($[Br_2]_0$ =0.0250 mM) of *N,N*-dimethylaniline (0.500 mM) at 25°C.

Exp. #	pH	k_1^{obs}, s^{-1}	k_2^{obs}, s^{-1} M^{-1}
IT-206M	0.465	2.66	1.56×10^4
IT-201M	0.561	4.42	2.58×10^4
IT-205M	0.682	5.90	3.45×10^4
IT-200M	0.851	9.90	5.79×10^4
IT-199M	1.14	20.6	1.21×10^5
IT-204M	1.43	42.0	2.46×10^5
IT-203M	1.82	108	6.33×10^5
IT-202M	2.14	191	1.12×10^6

Table B1.3. Raw Data for the Bromination of 2-Aminopyridine (1.00 mM) at 25°C.

Exp. #[a]	pH	k_1^{obs}, s^{-1}	k_2^{obs}, s^{-1} M^{-1}
IT-103M	0.153	4.60×10^{-4}	1.33
IT-96M	0.561	1.30×10^{-3}	3.89
IT-113M	0.561	3.00×10^{-3}	8.44
IT-111M	0.852	3.80×10^{-3}	10.9
IT-110M	1.14	8.50×10^{-3}	24.3
IT-99M	1.44	1.52×10^{-2}	44.5
IT-102M	1.84	3.95×10^{-2}	115
IT-101M	2.16	9.29×10^{-2}	272
IT-100M	2.45	2.86×10^{-1}	836
IT-105M	3.11	1.04	3.04×10^{3}
IT-104M	3.71	2.68	7.84×10^{3}
IT-112M	4.01	9.06	2.58×10^{4}
IT-106M	4.47	22.5	6.60×10^{5}
IT-107M	5.01	71.4	2.10×10^{5}

[a] The $[Br_2]_o$ used was 0.0500 mM for all the experiments with the exception of IT-110M through IT-113M where0.0250 mM was used instead.

Table B1.3.1 Raw Data for the Dependence of k_1^{obs} on [2-aminopyridine] using $[Br_2]_0$ = 0.0500 mM at 25°C.

Exp. #	[2-APy] - $[Br_2]_o$, mM	k_1^{obs}, s^{-1}
IT-109M[a]	0.200	3.85
	0.450	10.1
	0.950	21.5

[a] The experiments were performed at a pH of 4.43.

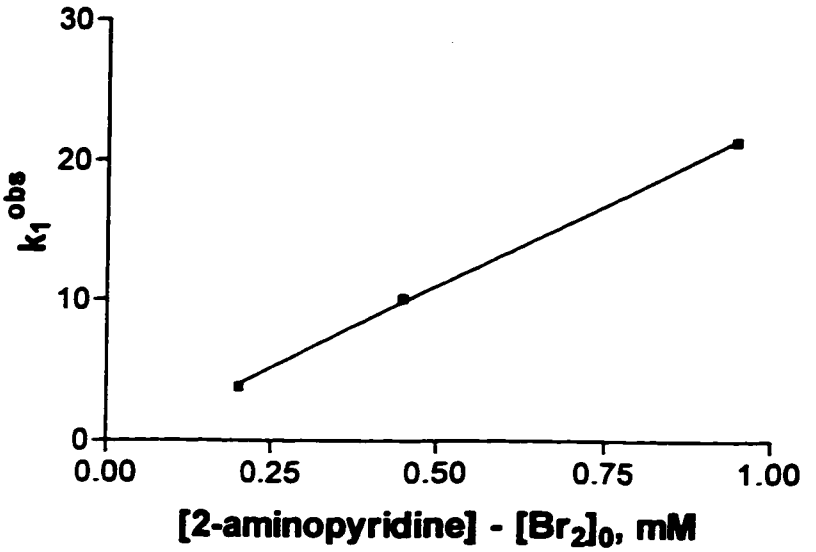

Figure B1.3.1 Dependence of k_1^{obs} on the 2-aminopyridine concentration at pH=4.43.

Table B1.3.2 Raw Data for the Dependence of the Amplitude on the $[Br_2]_o$ at 25°C, for the bromination of 2-aminopyridine.

Exp. #	$[Br_2]_o$, mM	Amplitude
IT-108M[a]	0.0125	0.192
	0.0250	0.475
	0.0500	0.747

[a] The experiments were performed at a pH of 4.41.

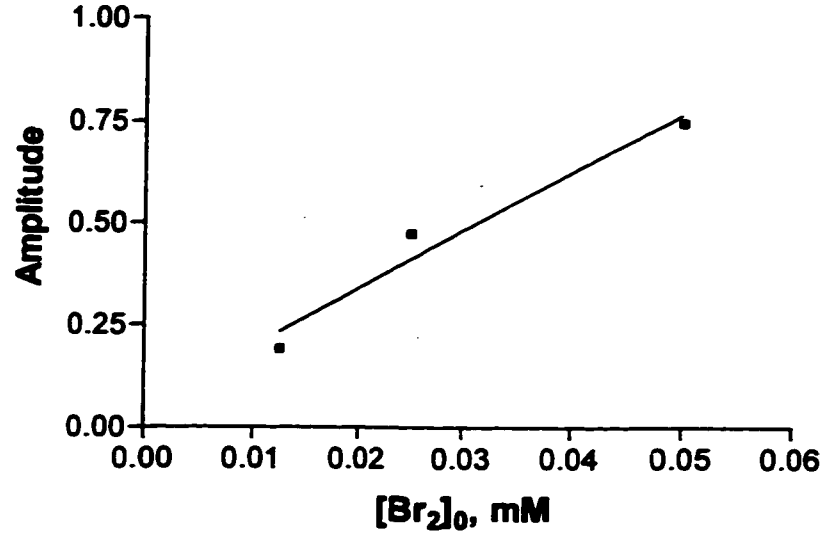

Figure B1.3.2 Dependence of the amplitude on the bromine concentration at pH=4.407 for the bromination of 2-aminopyridine.

Table B1.4. Raw Data for the Bromination ($[Br_2]_0$ = 0.0250 mM) of 2-dimethylaminopyridine (1.00 mM) at 25°C.

Exp. #	pH	k_1^{obs}, s^{-1}	k_2^{obs}, s^{-1} M^{-1}
IT-180M	0.465	1.43×10^{-2}	40.8
IT-187M	0.852	5.86×10^{-2}	167
IT-179M	1.14	8.60×10^{-2}	245
IT-178M	1.44	2.00×10^{-1}	570
IT-177M	1.84	5.23×10^{-1}	1.49×10^{3}
IT-181M	2.16	1.04	2.97×10^{3}
IT-182M	2.55	5.13	1.46×10^{4}
IT-185M	3.07	9.60	2.74×10^{4}
IT-183M	3.40	76.9	2.19×10^{5}
IT-186M	4.06	342	9.76×10^{5}
IT-182M	4.68	206	5.87×10^{5}

Table B1.4.1 Raw Data for the Dependence of k_1^{obs} on [2-dimethylaminopyridine] using $[Br_2]_0$ = 0.0500 mM at 25°C.

Exp. #	[2-DAPy] - $[Br_2]_0$, mM	k_1^{obs}, s^{-}
IT-187M[a]	0.975	0.0590
	1.98	0.0970
	3.98	0.210

[a] The experiments were performed at a pH of 0.865.

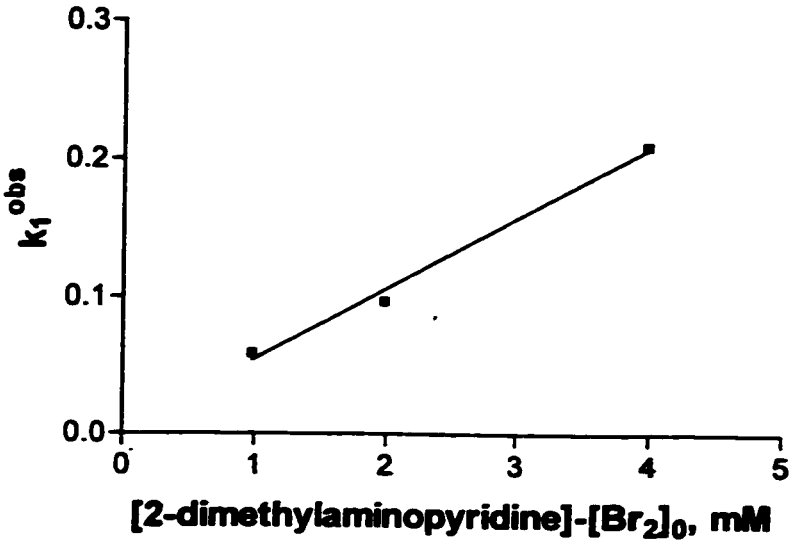

Figure B1.4.1 Dependence of k_1^{obs} on the 2-dimethylaminopyridine concentration at pH= 0.865.

Table B1.5. Raw Data for the Bromination of 2-Amino-4,6-dimethylpyrimidine (1.00 mM) at 25°C.

Exp. #[a]	pH	k_1^{obs}, s^{-1}	k_2^{obs}, s^{-1} M^{-1}
IT-135M	0.153	4.29×10^{-2}	122
IT-138M	0.257	5.85×10^{-2}	167
IT-136M	0.465	9.71×10^{-2}	277
IT-137M	0.561	1.28×10^{-1}	364
IT-129M	1.14	7.10×10^{-1}	2.00×10^{3}
IT-149M	1.44	1.49	4.25×10^{3}
IT-130M	2.16	8.51	2.43×10^{4}
IT-132M	3.09	116	3.31×10^{5}

[a] The $[Br_2]_o$ used was 0.0250 mM for all the experiments with the exception of IT-129M where 0.0126 mM was used instead.

Table B1.5.1 Raw Data for the Dependence of k_1^{obs} on [2-amino-4,6-dimethylpyrimidine] using $[Br_2]_0$ = 0.0500 mM at 25°C.

Exp. #	[2-ADP] - $[Br_2]_o$, mM	k_1^{obs}, s^{-1}
IT-149M[a]	0.480	0.835
	0.970	1.49
	2.00	2.80

[a] The experiments were performed at a pH of 1.44.

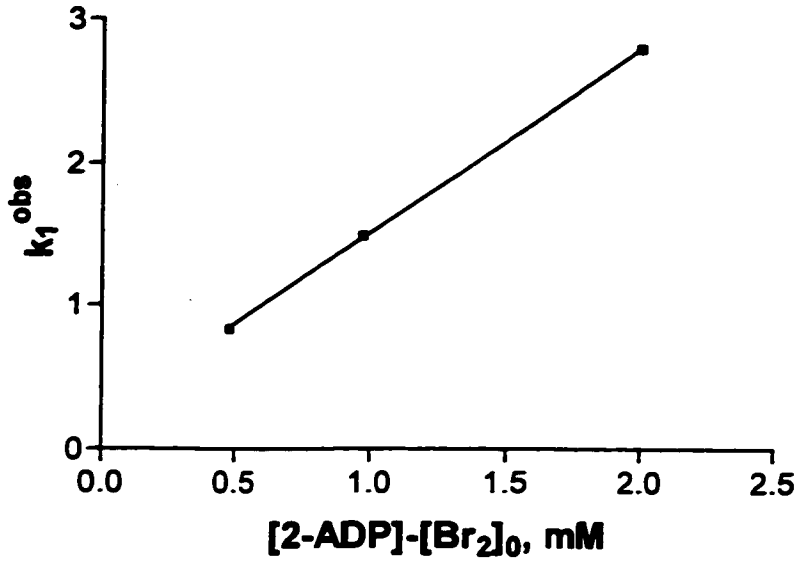

Figure B1.5.1 Dependence of k_1^{obs} on the 2-amino-4,6-dimethylpyrimidine concentration minus the bromine concentration at pH=1.429.

Table B1.6. Raw Data for the Bromination of 2-Aminopyrimidine (1.00 mM) at 25°C.

Exp. #	$[Br_2]_0$, M	pH	k_1^{obs}, s^{-1}	k_2^{obs}, s^{-1} M^{-1}
IT-91M	5×10^{-5}	0.153	0.372	1.09×10^3
IT-90M	5×10^{-5}	0.73	0.419	1.23×10^3
IT-89M	5×10^{-5}	0.88	0.449	1.31×10^3
IT-88M	5×10^{-5}	0.852	0.488	1.43×10^3
IT-87M	5×10^{-5}	1.14	0.455	1.33×10^3
IT-86M	5×10^{-5}	1.44	0.488	1.43×10^3
IT-147M	2.5×10^{-5}	1.84	0.565	1.61×10^3
IT-39M[a]	2.5×10^{-5}	2.16	0.566	1.61×10^3
IT-76M[a]	5×10^{-5}	2.19	0.420	1.23×10^3
IT-79M	5×10^{-5}	2.27	0.520	1.52×10^3
IT-142M	2.5×10^{-5}	2.58	1.05	3.00×10^3
IT-85M	5×10^{-5}	2.68	1.02	3.00×10^3
IT-82M	5×10^{-5}	2.89	1.38	4.04×10^3
IT-70M	5×10^{-5}	2.92	1.88	5.49×10^3
IT-68M	5×10^{-5}	3.33	3.29	9.64×10^3
IT-69M	5×10^{-5}	3.72	5.33	1.56×10^4
IT-65M	5×10^{-5}	3.98	7.34	2.15×10^4
IT-64M	5×10^{-5}	4.30	7.70	2.25×10^4
IT-73M	5×10^{-5}	4.45	7.64	2.24×10^4
IT-66M	5×10^{-5}	4.70	7.94	2.33×10^4
IT-67M	5×10^{-5}	4.97	7.70	2.26×10^4
IT-71M	5×10^{-5}	5.36	7.46	2.20×10^4
IT-72M	5×10^{-5}	5.62	7.52	2.23×10^4

[a] These experiments were not taken into account when calculating the pK_a value.

Table B1.6.1 Raw Data for the Dependence of k_1^{obs} on [2-aminopyrimidine] using $[Br_2]_0$ = 0.0500 mM at 25°C.

Exp. #	[2-AP] - $[Br_2]_0$, mM	k_1^{obs}, s^{-1}
IT-93M[a]	0.450	0.229
	0.950	0.493
	1.95	0.857
IT-94M[b]	0.450	4.78
	0.950	8.23
	1.95	13.5

[a] The experiments were performed at a pH of 0.852.
[b] The experiments were performed at a pH of 4.34.

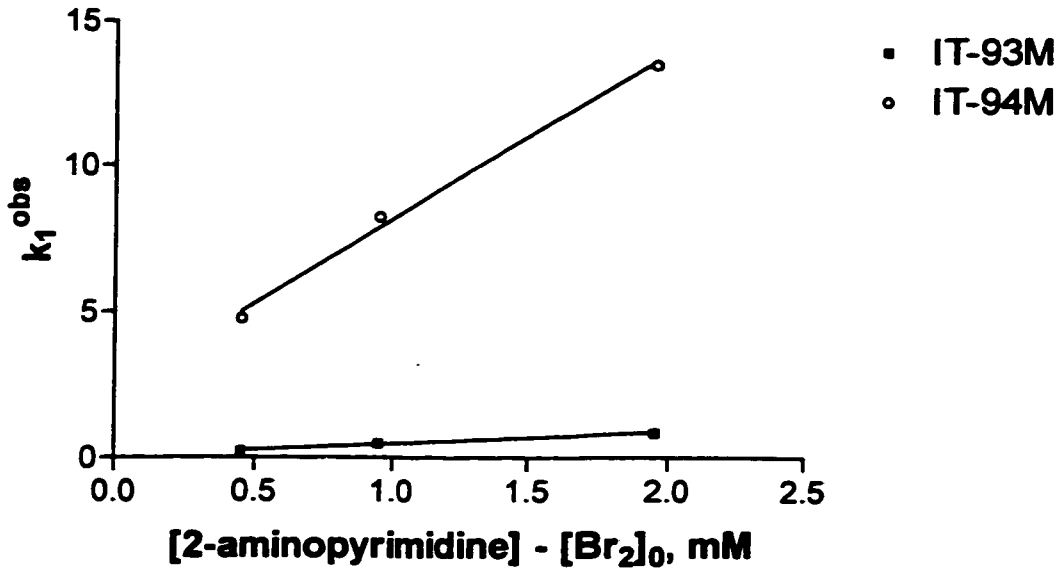

Figure B1.6.1 Dependence of k_1^{obs} on the 2-aminopyrimidine concentration at pH=0.852 for experiment IT-93M and a pH of 4.34 for experiment IT-94M.

Table B1.6.2 Raw Data for the Dependence of the Amplitude on the $[Br_2]_0$ for the Bromination of 2-aminopyrimidine at 25°C.

Exp. #	$[Br_2]_o$, mM	Amplitude
IT-95M[a]	0.0125	0.255
	0.0250	0.548
	0.0500	1.03

[a] The experiments were performed at a pH of 1.44.

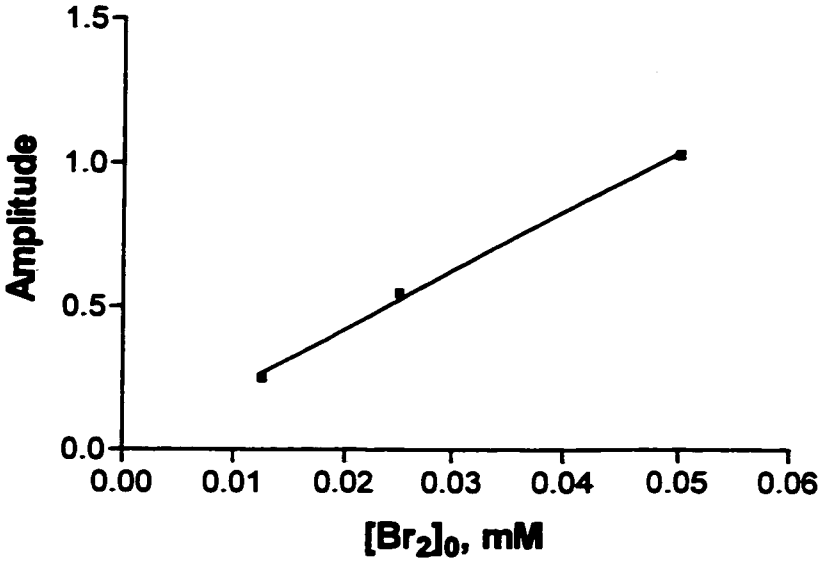

Figure B1.6.2 Dependence of the amplitude on the bromine concentration at pH=0.852 for the bromination of 2-aminopyrimidine.

Table B1.7. Raw Data for the Bromination ($[Br_2]_0$ =0.0250 mM) of 1,2-dihydro-2-imino-1-methylpyrimidine (0.250 mM) at 25°C.

Exp. #	pH	k_1^{obs}, s^{-1}	k_2^{obs}, s^{-1} M^{-1}
IT-119M	0.152	6.15×10^{-2}	759
IT-124M	0.465	9.43×10^{-2}	1.17×10^{3}
IT-118M	1.14	8.40×10^{-2}	1.04×10^{3}
IT-114M	2.13	7.14×10^{-2}	882
IT-115M	2.95	2.54×10^{-2}	313
IT-116M	3.85	4.65×10^{-4}	5.75
IT-123M	3.90	4.99×10^{-4}	6.17
IT-117M	4.86	4.81×10^{-3}	59.6
IT-121M	4.96	1.11×10^{-2}	137
IT-125M	5.56	1.01×10^{-1}	1.26×10^{3}
IT-128M	5.85	2.56	3.24×10^{4}
IT-126M	6.09	14.5	1.86×10^{5}
IT-127M	6.32	20.4	2.70×10^{5}
IT-122M	6.77	46.7	6.96×10^{5}

Table B1.7.1 Raw Data for the Dependence of k_1^{obs} on [1,2-dihydro-2-imino-1-methylpyrimidine] using $[Br_2]_0$ = 0.0500 mM at 25°C.

Exp. #	[M2A] - $[Br_2]_o$, mM	k_1^{obs}, s^{-1}
IT-124M[a]	0.100	0.0490
	0.220	0.0940
	0.480	0.175
IT-125M[b]	0.100	0.0520
	0.220	0.101
	0.480	0.156

[a] The experiments were performed at a pH of 0.465.
[b] The experiments were performed at a pH of 5.56.

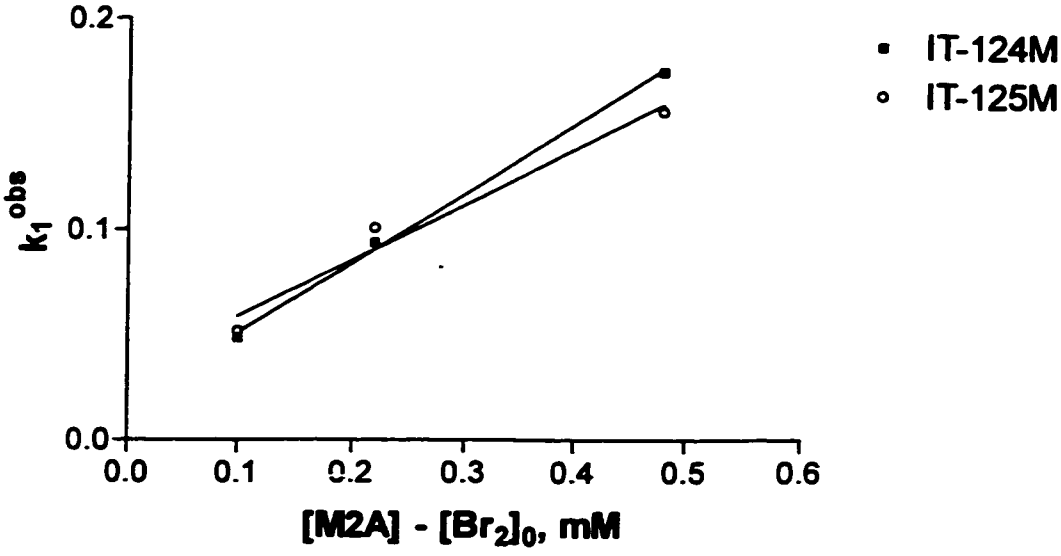

Figure B1.7.1 Dependence of k_1^{obs} on the 1,2-dihydro-2-imino-1-methylpyrimidine concentration minus the bromine concentration at pH=0.465 for experiment IT-124M and a pH of 5.56 for experiment IT-125M.

Table B1.8. Raw Data for the Bromination ($[Br_2]_b$ = 0.0250 mM) of Synthesized 1,2-dihydro-2-imino-1-methylpyrimidine (0.250 mM) at 25°C.

Exp. #	pH	k_1^{obs}, s^{-1}	k_2^{obs}, s^{-1} M^{-1}
IT-157M	0.152	7.40×10^{-2}	914
IT-154M	0.465	7.95×10^{-2}	982
IT-153M	0.852	9.09×10^{-2}	1.12×10^{3}
IT-150M	1.14	1.06×10^{-1}	1.30×10^{3}
IT-151M	1.43	8.05×10^{-2}	994
IT-152M	2.13	6.47×10^{-2}	799
IT-156M	2.70	4.76×10^{-2}	588
IT-162M	4.38	3.40×10^{-3}	42
IT-159M	4.46	3.12×10^{-3}	39
IT-163M	4.69	8.46×10^{-3}	105
IT-160M	4.92	2.19×10^{-2}	272
IT-164M	5.14	5.51×10^{-2}	683
IT-167M	5.28	8.46×10^{-2}	1.05×10^{3}
IT-170M	5.41	1.42×10^{-1}	1.77×10^{3}
IT-172M	5.45	2.06×10^{-1}	2.57×10^{3}
IT-171M	5.87	1.55×10^{-1}	1.98×10^{3}
IT-173M	5.87	2.13×10^{-1}	2.70×10^{3}
IT-168M	5.34	27.5	3.42×10^{5}
IT-169M	5.67	25.5	3.21×10^{5}
IT-166M	5.80	12.6	1.59×10^{5}
IT-175M[a]	5.81	18.1 5.67×10^{-1}	2.29×10^{5} 7.16×10^{3}
IT-176M[a]	6.21	20.4 2.04×10^{-1}	2.66×10^{5} 2.66×10^{3}
IT-174M[a]	6.42	50.5 5.56×10^{-2}	6.81×10^{5} 749

[a] Two different rates were observed, a fast rate and a slow rate.

Bromination of Aniline File: br2anili.wk4

Date: 02-Feb-99

			8.49	Albert & Serjeant
K1 =	0.0562	M	pKa of HOBr =	8.69 CRC Handbook
K2 =	9.60E-09	M^2	Ka of HOBr =	2.06E-09 CRC Handbook
K1*K2 =	5E-10	M^3		

Expt. #	pH	[H+]	[KBr]	[substrate]	[Br2]t	k1-obs	k2-app	k2-obs	log k2-obs	log k2-calc
IT-190M	0.465	3.43E-01	0.100	1.00E-03	2.50E-05	11.31	11600	32241	4.508	4.646
IT-195M	0.561	2.75E-01	0.100	1.00E-03	2.50E-05	17.18	17621	48974	4.690	4.742
IT-194M	0.683	2.07E-01	0.100	1.00E-03	2.50E-05	24.99	25631	71237	4.853	4.864
IT-189M	0.852	1.41E-01	0.100	1.00E-03	2.50E-05	35.12	36021	100114	5.000	5.033
IT-193M	1.14	7.21E-02	0.100	1.00E-03	2.50E-05	80.14	82195	228449	5.359	5.323
IT-192M	1.44	3.66E-02	0.100	1.00E-03	2.50E-05	155.7	159692	443843	5.647	5.618
IT-191M	1.84	1.44E-02	0.100	1.00E-03	2.50E-05	308.4	316308	879135	5.944	6.021
IT-198M	2.16	6.92E-03	0.100	1.00E-03	2.50E-05	814.8	835692	2322701	6.366	6.340

k2 =		1/(M/s)	k2' =	5.77E+08	1/(M/s)
pKa =	4.58		Ka =	2.63E-05	M

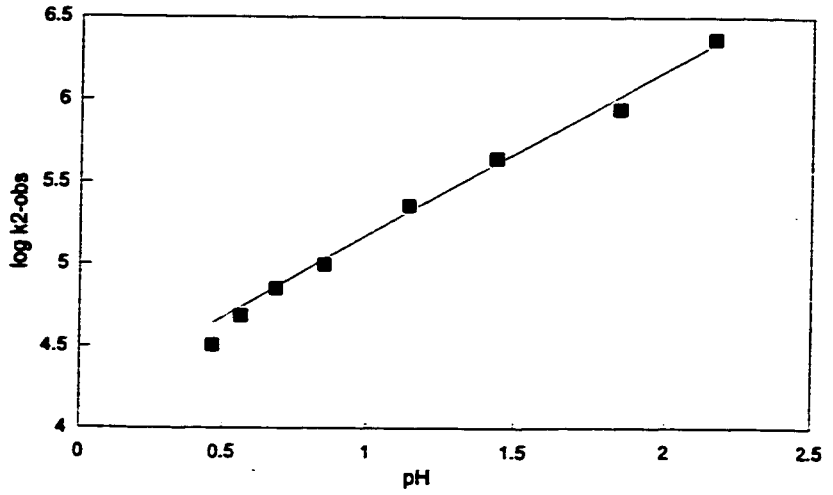

Scheme B1 Lotus 1-2-3 spreadsheet for the bromination of aniline.